AD-A146 188 AN INVESTIGATION OF A CRYOGENIC MATRIX ISOLATION APPROACH FOR CHARACTERIZ..(U) IIT RESEARCH INST CHICAGO IL A SNELSON JUL 84 CRDC-CR-84050 DAAK11-81-K-0007 1/2

UNCLASSIFIED F/G 7/4 NL

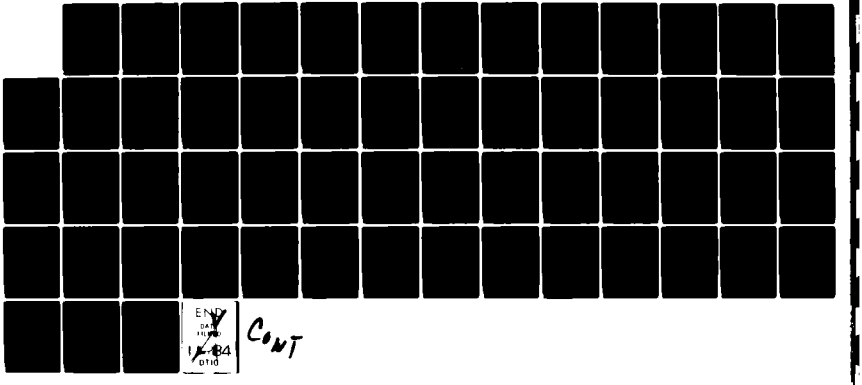

CONT

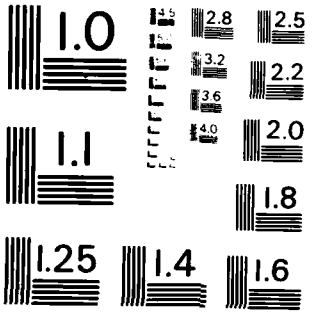

10

CRDC-CR-84050

AN INVESTIGATION OF A CRYOGENIC MATRIX ISOLATION APPROACH FOR CHARACTERIZING PHOSPHORUS ACID AEROSOL

FINAL REPORT ON
IITRI CONTRACT NO. C06540

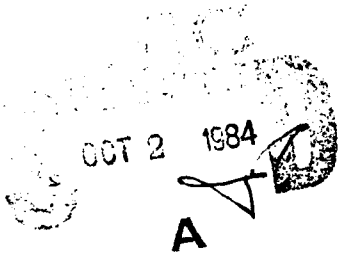

by ALAN SNELSON

IIT RESEARCH INSTITUTE
10 West 35th Street
Chicago, Illinois 60616

CONTRACT NO. DAAK11-82-C-0149

JULY 1984

US Army Armament, Munitions & Chemical Command
Aberdeen Proving Ground, Maryland 21010

Disclaimer

The findings in this report are not to be contrued as an official Department of the Army position unless so designated by other authorizing documents.

Disposition

For classified documents, follow the procedures in DOD 5200.1-R, Chapter IX, or DOD 5220.22-M, "Industrial Security Manual," paragraph 19. For unclassified documents, destroy by any method which precludes reconstruction of the document.

Distribution Statement

Approved for public release; distribution unlimited.

UNCLASSIFIED

SECURITY CLASSIFICATION OF THIS PAGE (When Data Entered)

REPORT DOCUMENTATION PAGE		READ INSTRUCTIONS BEFORE COMPLETING FORM
1. REPORT NUMBER CRDC-CR-84050	2. GOVT ACCESSION NO. AD-A144 139	3. RECIPIENT'S CATALOG NUMBER
4. TITLE (and Subtitle) An Investigation of a Cryogenic MATRIX Isolation Approach for Characterizing Phosphorus Acid Aerosol		5. TYPE OF REPORT & PERIOD COVERED Final Report Sep 1981-Jun 1983 6. PERFORMING ORG. REPORT NUMBER
7. AUTHOR(s) Alan Snelson		8. CONTRACT OR GRANT NUMBER(s) DAAK11-81-K0007
9. PERFORMING ORGANIZATION NAME AND ADDRESS IIT Research Institute 10 West 35th Street Chicago, Illinois 60616		10. PROGRAM ELEMENT, PROJECT, TASK AREA & WORK UNIT NUMBERS
11. CONTROLLING OFFICE NAME AND ADDRESS Issued by Commander Chemical Research and Development Center Attn: DRSMC-CLJ-IR(A) Aberdeen Proving Ground, Maryland 21010		12. REPORT DATE July 1984 13. NUMBER OF PAGES 58
14. MONITORING AGENCY NAME & ADDRESS (if different from Controlling Office) Commander Chemical Research and Development Center Attn: DRSMC-CLB-PS Aberdeen Proving Ground, Maryland 21010		15. SECURITY CLASS. (of this report) Unclassified 15a. DECLASSIFICATION DOWNGRADING SCHEDULE NA

16. DISTRIBUTION STATEMENT (of this Report)

Approved for public release; distribution unlimited

17. DISTRIBUTION STATEMENT (of the abstract entered in Block 20, if different from Report)

A

18. SUPPLEMENTARY NOTES

This study was sponsored by the Army Smoke Research Program, Chemical Research and Development Center. Contract Project Officer: Dr. Edward W. Stuebing, DRSMC-CLB-PS, 301-671-3089.

19. KEY WORDS (Continue on reverse side if necessary and identify by block number)

Phosphorus smoke composition
Phosphorus acid aerosol
Cryogenic sampling
Infrared spectral analysis
Vibrational assignment for H_3PO_2,
IR spectra of H_3PO_3, H_3PO_4, $H_4P_2O_7$, $(HPO_3)n$, P_2O_5

20. ABSTRACT (Continue on reverse side if necessary and identify by block number)

A matrix isolation cyrostat has been adapted to sample gas streams containing aerosols for the latters subsequent analysis by infrared spectroscopy. The aerosol sampling was made in basically one of two modes: (1) the aerosol and its carrier gas were both condensed at 10K on the IR-transmitting surface, or (2) the aerosol alone was condensed on the IR-transmitting surface maintained at a temperature insufficient to condense the carrier gas. IR spectra of the condensed air + aerosol, or the aerosol alone, were then obtained. By suitably

UNCLASSIFIED

DD FORM 1 JAN 73 1473

SECURITY CLASSIFICATION OF THIS PAGE (When Data Entered)

20. (Cont'd)

varying the temperature of the IR-transmitting surface, the air was distilled off leaving the aerosol behind. For aqueous aerosols containing none volatile solutes, the water could be partially or completely removed by raising the temperature of the condensed material to approximately 200K, followed by recooling to 10K for spectral analyses.

The new aerosol sampling and analytical approach has been applied to determine the composition of smokes resulting from burning red or white phosphorus in air. Reference spectra of aqueous aerosols of the following phosphorus acids were obtained: H_3PO_2, D_3PO_2, H_3PO_3, H_3PO_4, $H_4P_2O_7$, polyphosphoric acids, and $(HPO_3)n$. The cryogenic spectra of these aqueous acids showed improved spectral resolution compared to their solution counterparts at ambient temperature. The dehydration procedure noted above resulted in spectra of much improved quality. For H_3PO_2 and D_3PO_2, isotope frequency shift data were used to make a new vibrational assignment for these species.

Comparison of the reference spectra of cryogenic phosphorus acid with those of the aerosol obtained from burning red and white phosphorus in air at $\simeq$ 50% relative humidity indicate the latter did not correspond to any one individual acid or to a simple mixture thereof. A few experiments were made in which phosphorus was burned in air at relative humidities from 0% to 25%, with residence times in the reactor before sampling of from 1.2 to 10 seconds. The spectral data so obtained indicated that the initial hydrolysis product had a strong absorption feature at $\simeq$7.5 μ, which moved to longer wavelengths as the extent of hydrolysis increased. The origin of this band (not found in any of the reference spectra) and its relation to the anomalous 8 μ feature of phosphorus smokes is discussed.

PREFACE

The work described in this report was authorized under Contract No. DAAK11-81-K0007. This work was started in September 1981 and completed in June 1983.

The use of trade names in this report does not constitute an official endorsement or approval of the use of such commercial hardware or software. This report may not be cited for purposes of advertisement.

Acknowledgments

The enthusiastic support of Dr. Edward W. Stuebing during the course of the study is gratefully acknowledged.

A-1

CONTENTS

LIST OF FIGURES

LIST OF FIGURES (Cont)

AN INVESTIGATION OF A CRYOGENIC MATRIX ISOLATION APPROACH FOR CHARACTERIZING PHOSPHORUS ACID AEROSOL

1. INTRODUCTION

The US Army has a strong interest at the present time in the use of smokes as obscuration agents on the battlefield. With the increasing sophistication of the so-called "smart weapons," the demands on the obscuration properties of the smokes have become more severe insomuch that protection is not only needed in the visible region of the spectrum but also in the infrared and microwave ranges. Currently, the only smokes in the Army inventory that perform reasonably well in the visible and IR are those generated by burning white or red phosphorus munitions. For this reason these smokes are of importance. The obscuration properties of smokes are reasonably well understood in terms of the scattering and absorption properties of the aerosol particulates constituting the smoke.[1,2] Taking the simplest case, that of spherical particles, obscuration properties can be calculated theoretically if the following parameters are defined for the aerosol:

r - the radius of the particle,

x - the wavelength of the electromagnetic radiation,

m - the complex refractive index of the aerosol particle. m is written as a complex number $m = n(1-ik)$, which separates the refraction term n from the absorption term nk,

n' - the number density of the particles.

Of particular concern in this study is the problem of defining a value of m for the phosphorus smoke aerosol. In principle, this is a straightforward task; all that is needed are the refractive indices and absorption coefficients of the aerosol material as a function of wavelength. These properties may be measured relatively easily on samples of the bulk material, providing its composition can be defined (i.e., the same as that of the aerosol of interest). Unfortunately, for the phosphorus smokes, the composition of aerosol is not well defined. US Army studies[3-6] have shown that calculated extinction coefficients for the phosphorus smoke aerosol, based on the assumption of an aerosol composed of an aqueous phosphoric acid solution, do not reproduce experimentally determined values accurately. In

particular, phosphorus smokes have a strong absorption at ≈ 8.0 μm, which an artificially produced phosphoric acid aerosol does not exhibit.

In most of the early studies on phosphorus smoke aerosols,[7-12] three reactions were taken as sufficient to describe the phosphorus smoke formation process.

$$P_4 + 5O_2 \rightarrow P_4O_{10}$$
$$P_4O_{10} + 6H_2O \rightarrow 4H_3PO_4$$
$$H_3PO_4 + nH_2O \rightarrow H_3PO_4nH_2O$$

In a later study,[13] an attempt was made to chemically characterize the phosphorus smoke aerosol. The acid component of the aerosol was described as being well represented by a mixture of tetrametaphosphoric acid $(HPO_3)_4$ and pyrophosphoric acid $(H_4P_2O_7)$ in a 1:6 ratio. In this study, pure red phosphorus was burned in air to produce the aerosol. Collected aerosol was subjected to ^{31}P and ^{1}H NMR analyses. From the observed resonances, the above acids were inferred to be present. After standing overnight, the collected aerosol was judged to contain only phosphoric acid, based on the NMR spectrum. Aerosol acid titration data were used to infer the $(HPO_3)_4$ to $H_4P_2O_7$ ratio noted above.

In a recent study in this laboratory,[14] felt wedges saturated with white phosphorus were burned in air and the resultant aerosol trapped at liquid nitrogen temperature and subjected to chemical analyses using high pressure ion exchange liquid chromatography. The aerosol appeared to consist of a mixture of polyphosphoric acids, $H_{n+2}P_nO_{3n+1}$. Individual polymers up to n = 8 were identified and constituted about 60% of the aerosol. The remaining 40%, probably polyphosphoric acids with n > 8, were not resolved experimentally. Conversion of the higher polymers to phosphoric acid was not complete after 8 days standing at ambient temperature.

It is not clear at this point why the results of these two studies are not in better agreement with respect to the aerosol composition. It is possible that aerosol formed from burning pure red phosphorus in air (first study) is different from that obtained by burning the white phosphorus felt wedge material (second study). Alternatively, the collection and subsequent handling of the

aerosol may have caused chemical changes to take place such that the original aerosol composition was modified. Unfortunately, these types of difficulties are commonplace when attempting to collect and chemically analyze potentially reactive aerosols. In an attempt to overcome these difficulties, the present program was initiated to investigate a cryogenic sampling and infrared analytical approach.

2. EXPERIMENTAL

The approach used in the present study was basically a simple modification of the well known matrix isolation technique which utilizes low temperature inert gas matrices to trap reactive chemical radicals or unstable high temperature species.[15] In the present context, the aerosol may be regarded as the "reactive" material to be sampled and isolated, and the ambient gas phase containing the aerosol, the low temperature matrix gas. Characterization of the aerosol chemically is then made via its infrared spectrum. In practice, it was found that useful results could also be obtained by directly freezing the aerosol onto the low temperature sampling surface without the "matrix gas." The experimental setup used in the present study will be described.

The cryostat used was based on an Air Products Displex CS202 closed-cycle helium refrigerator. Its salient features are shown in Figure 1. The unit routinely achieved a low temperature of 8-10K at the copper block containing the cesium iodide window on which the aerosol and carrier gas were deposited. The cooled window could be rotated to be perpendicular either to the aerosol sampling port during deposition or to the IR analyzing beam of the spectrophotometer for spectral analyses. An electrical heater, attached to the copper block housing the window, allowed the latter's temperature to be varied from 10K to slightly above ambient. The gas stream containing the aerosol was directed at the cooled window through a 0.635 cm OD stainless-steel tube terminated at the deposition end by a stainless-steel plate 0.01 cm thick containing a hole 0.034 cm in diameter. The perforated plate was ≈ 3 cm from the surface of the cooled deposition window. At 1 atm. pressure this inlet system allowed 100 cm^3 sec^{-1} and 60 cm^3 sec^{-1} of helium and air carrier gases, respectively, to enter the cryostat. External to the cryostat, the stainless-steel tube was connected to a 1/8-inch "Nupro" ball valve, which was used to isolate the

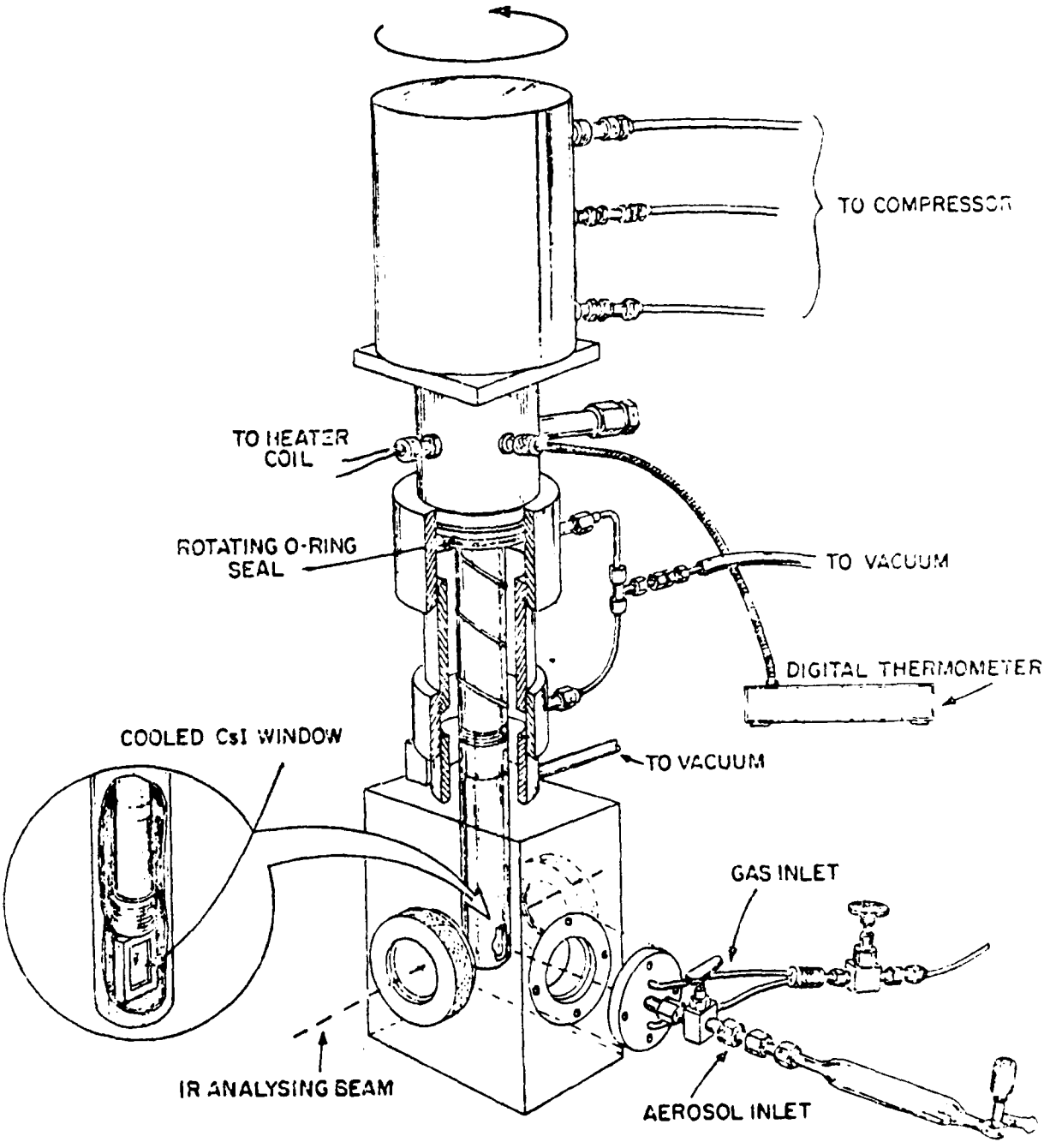

Figure 1. Cryogenic Aerosol Sampler

cryostat from a glass aerosol/gas storage volume. An all glass and teflon high-vacuum valve isolated the other end of the storage volume from a glass tube ≈14 mm ID through which the aerosol gas stream of interest was passed. The cryostat was continuously evacuated by a conventional oil diffusion and mechanical pump system.

The experimental arrangements used for generating and sampling the various aerosol gas streams are shown in Figure 2. Aerosol containing gas streams of specific aqueous phosphorus acids were prepared using a De Vilbis nebulizer loaded with a suitable aqueous solution of the acid. Either Air Products "Zero Grade" air or helium were used as carrier gases. Gas flow rates through the nebulizer were ≈ 400 cm^3 sec^{-1} resulting in aerosol loadings of ≈ 1-4 x 10^{-6} $g.cm^{-3}$. The latter was determined gravimetrically by collecting the aerosol from a known volume of carrier gas on Gellman Type A glass fiber filters. Particle size measurements were made on some phosphorus acid aerosols generated using the De Vilbis nebulizer which indicated number mean particle diameters in the 0.4-to 0.6-μm range under conditions where aerosol coagulation was minimal. (These experiments and the results are presented in the Appendix.)

Phosphorus smoke aerosols were produced by burning samples of red or white phosphorus contained in an alumina boat (8 cm long, 1 cm wide, 1 cm deep) housed in a quartz reactor tube 6.5 cm ID and 27 cm long. The ends of the reactor were sealed with rubber stoppers containing inlets and outlets for the carrier gas. Prior to burning the red phosphorus, the sample was introduced into the reactor, the residual atmosphere flushed out with the zero air, and the sample then ignited by gentle external heating of the quartz reactor with a gas-oxygen flame. The white phosphorus was stored under water prior to use. A few small pieces of the white phosphorus were quickly removed from the water, introduced into the alumina boat in the reactor, and the whole assembly flushed with dry helium until the sample was dry. The sample was ignited by replacing the helium carrier gas with air. Carrier gas flow rates through the reactor were varied to give residence times of ≈ 1 - 25 sec. The relative humidity of the carrier gas was controlled by mixing two gas streams in the desired ratios, one saturated with water vapor and the other completely dry.

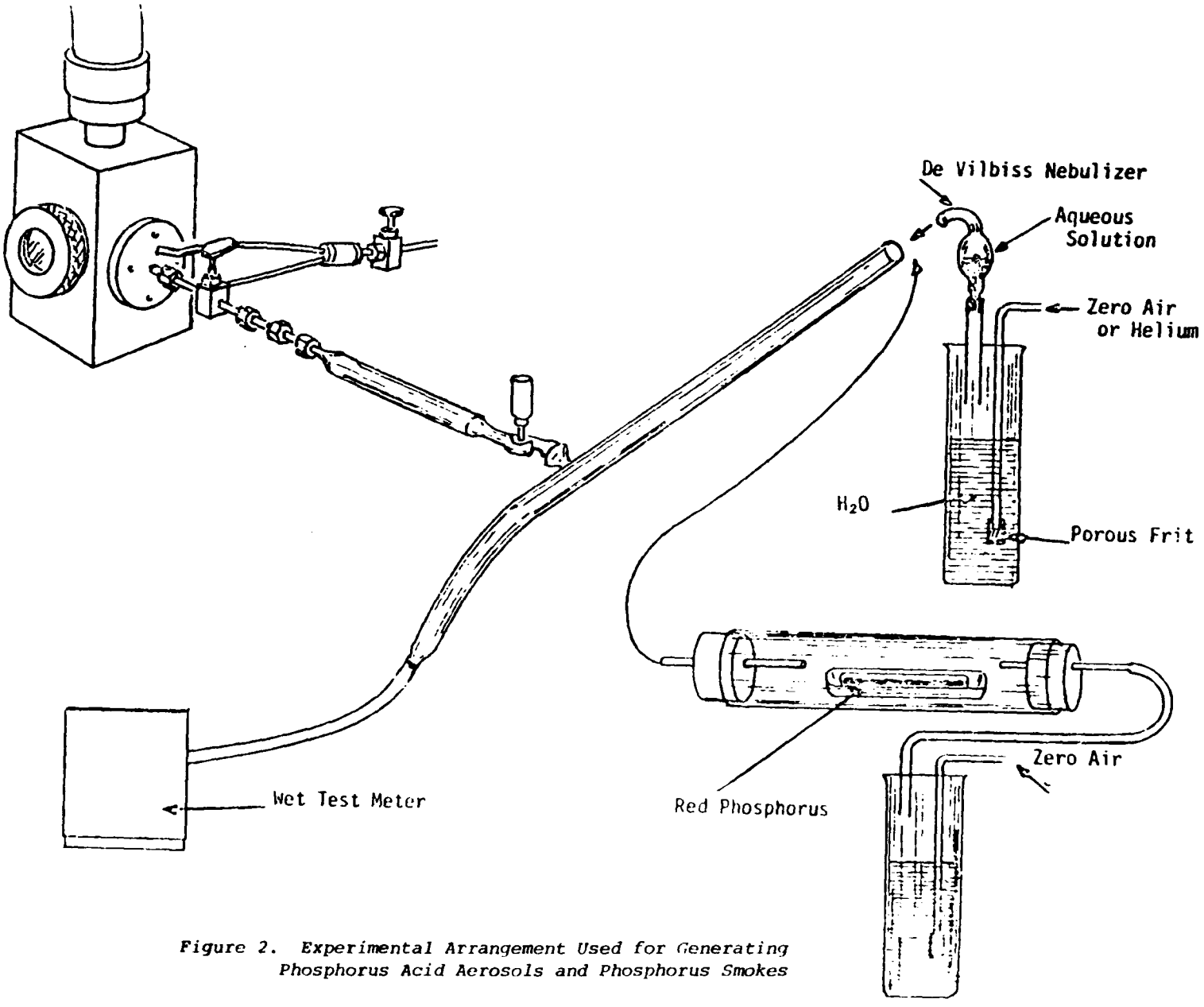

Figure 2. Experimental Arrangement Used for Generating Phosphorus Acid Aerosols and Phosphorus Smokes

The following phosphorus acids were obtained from Tridom Fluka and were used without further purification to obtain reference spectra: H_3PO_2, H_3PO_3, H_3PO_4, $H_4P_2O_7$, $(HPO_3)_n$ and polyphosphoric acid [$\simeq$ 60% $H_5P_3O_{10}$ + $\simeq$ 15% $H_4P_2O_7$+ $\simeq$ 10% $(HPO_3)_6$ + $\simeq$ 15% $(HPO_3)_x$]. Deuterated hypophosphorous acid, D_3PO_2, 98 atom % in D_2 was obtained from MSD Isotopes. Red phosphorus powder, 99% pure, was obtained from Aldrich Chemical Co. White phosphorus was obtained from the US Army, Fort Detrick. It was described as the material used in smoke munitions.

Spectra were recorded on a Perkin Elmer 283 spectrophotometer in the region from 4000 - 200 cm^{-1}. Spectra were recorded at a rate of $\simeq$ 1 cm^{-1} sec^{-1}. Frequency accuracy was checked against atmospheric water vapor bands and a polystyrene film standard. Reported frequencies are accurate to at least $\pm$ 3 cm^{-1}.

Cryogenic Aerosol Sampling And Manipulative Procedures

Aerosol sampling was effected in several ways which will be described.

(a) Aerosol Sampling And Trapping From the 20-ml Storage Volume In An Air Matrix At 10K. Spectra Recorded at 10K.

The cryostat and aerosol storage volume were evacuated, the cryostat cooled to 10K, and the aerosol carrier gas flow started. By suitable manipulation of the valves on the storage volume, 20 ml of aerosol laden gas stream were sampled into the storage volume. The stored aerosol gas sample was then introduced into the cryostat via the stainless-steel inlet probe with the cooled window perpendicular to the latter. The entire procedure was accomplished in $\simeq$ 10 sec. The spectrum of the trapped material on the window was quickly scanned to determine if sufficient material was present. If necessary, further depositions were made until sufficient optical density of the trapped material accrued and the spectrum was then obtained. When air was used as the carrier gas, a transient ($\simeq$ 10 - 15 sec.) window block temperature increase of $\simeq$ 2-3K occurred.

(b) Aerosol Sampling And Trapping From The 20 ml Storage Volume In An Air Matrix at 10K, Followed By Air Matrix Removal. Spectra Recorded At 10K.

The same procedures used in (a) were used with the following additions. After recording the spectrum of the aerosol trapped in the air matrix, the temperature of the window block was increased to ≈ 50-60K and the air matrix slowly pumped off (5-20 minutes depending on sample size). The window block was recooled to 10K and the spectrum recorded.

(c) Aerosol Sampling And Trapping From The 20-ml Storage Volume Using Air Carrier Gas At 70K. Spectra Recorded At 10K.

Essentially the same procedures used in (a) were followed with the exception that the window block was maintained at 70K during the initial deposition process. After deposition the window block was recooled to 10K and the spectrum recorded.

(d) Aerosol Sampling And Trapping From The 20-ml Storage Volume Using Air Carrier Gas Followed By Air And Water Removal From The Deposited Aerosol. Spectrum Recorded At 10K Or Higher.

Any of the procedures, (a), (b), or (c), were used initially. Water was removed from the aerosol (if aqueous) by raising the temperature of the window block to ≈ 220K for a few minutes. In practice, the water removal process was monitored by "locking" the spectrometer onto a water absorption band and monitoring the water disappearance via changes in the band intensity.

(e) Aerosol Sampling And Trapping Directly From A Carrier Gas Stream Using Short (1-5 sec) Sampling Periods Spectrum Recorded At 10K Or Higher

In this procedure the aerosol laden gas stream was sampled directly into the cryostat without using the 20-ml holding volume to store the sample. If isolation of the aerosol in an air matrix was required, 1-sec sampling periods were used. This resulted in a window block temperature rise of ≈ 5-8K, not sufficient to prevent efficient freezing of the air matrix. Longer sampling periods, up to 5 sec were also used, resulting in increases of window block temperature up to 20K. Under these conditions it is not certain how effectively the air condensed onto the window and, hence, how well the aerosol was isolated in the matrix. These larger deposition times were, therefore, only used when isolation of the aerosol in the air matrix was not required. Any of the previous procedures, (a), (b), (c), and (d), could be used in the direct sampling mode.

Helium was used in some experiments as the aerosol carrier gas. With the exception of being unable to trap the aerosol in a matrix, all of the procedures described when air was the carrier gas were used with helium.

3. RESULTS

3.1 Phosphorus Acids Reference Spectra - No Air Matrix.

In addition to developing the experimental procedures described for sampling the aerosol laden gas streams, a major portion of the program was devoted to obtaining cryogenic spectra of known phosphorus acid aerosols (currently not available in the literature). These spectra would be used in the identification of phosphorus acids in the aerosols generated by burning red or white phosphorus in air and similarly cryogenically sampled.

Initially in these studies, air was used as the carrier gas for generating the phosphorus acid aerosol. However, since the primary interest was to obtain the pure acid aerosol spectra at 10K without an air matrix, it was experimentally simpler to use helium as the carrier gas, deposit the aerosol at 10K, and record the spectra immediately at 10K, thus avoiding sample manipulation to remove the air using procedures (b) or (d) described earlier. In most of these experiments, between 100 to 400 ml of the aerosol gas stream was sampled in order to obtain sufficient aerosol for a good spectrum. The salient features of the pure phosphorus acid spectra will be presented.

3.1.1 H_3PO_2 - Hypophosphorus Acid.

Spectra at 10K of aqueous aerosols of hypophosphorus acid at three different concentrations are presented in Figure 3. For purposes of comparison, an inset shows the aqueous solution spectra at various concentrations obtained at ambient temperature. The spectrum (curve a) of 50 wt% H_3PO_2 is dominated by that of the water in the aerosol and shows only slight structure centered at about 1150 cm^{-1} attributable to the contained acid. As the concentration of the acid in the solution is increased (curves b and c), spectral features due to the acid appear, and contributions due to water diminish as expected. However, even at the highest acid

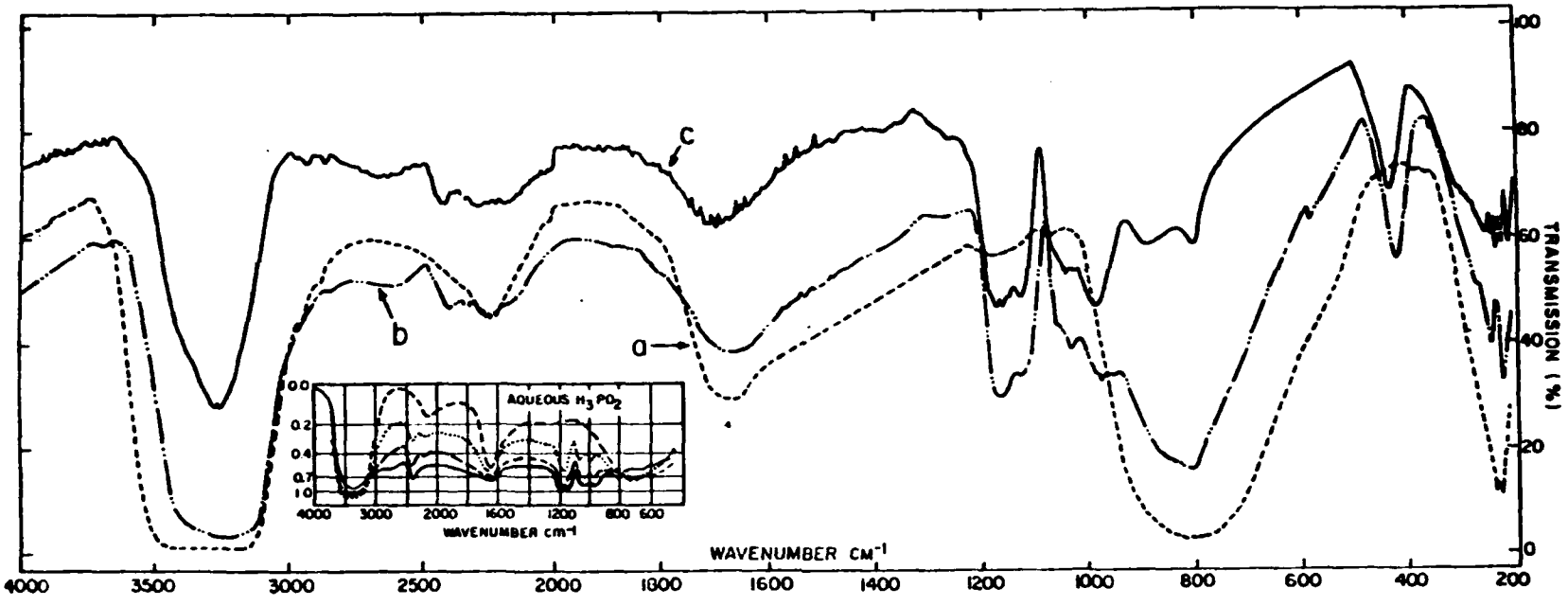

Figure 3. IR Spectra of Aqueous Hypophosphorous Acid Aerosol Generated Using Helium Carrier Gas, Deposited and Recorded at 10°K

(a) ≃50 wt% H_3PO_2; (b) ≃90 wt% H_3PO_2 and ≃98 wt% H_3PO_2.

concentration, the 3250 cm^{-1} feature due to water is still quite intense. In general, the 10K spectra of the aqueous hypophosphorous acid aerosol shows more and well-defined structure than the analogous ambient temperature aqueous solution spectra, demonstrating the advantage of the cryogenic approach when using IR spectral data for characterizing the aqueous aerosol. However, for the more dilute solutions, absorption band features due to water will predominate the spectrum, limiting the value of the IR analytical procedure for this acid at low concentration.

The results of a method to circumvent this difficulty are shown in Figure 4. In this approach the aerosol was deposited at 10K, as described above. The temperature of the window block was increased from 10K to 210K while monitoring the major water absorption band at $\simeq$ 3250 cm^{-1} as a function of time with the spectrometer locked onto this frequency. In the lower right hand corner of Figure 4 is a trace showing the change in intensity of the water vapor absorption band monitored at $\simeq$ 3250 cm^{-1} as a function temperature and time, indicating that at a temperature of $\simeq$ 170K water is beginning to be removed from the sample. At this temperature, the vapor pressure of pure water is $\simeq 2 \times 10^{-5}$ mm Hg and it appears that the water is being cyrogenically pumped from the heated window block to a cooler surface in the cryostat. The effect of this procedure is the dehydration of the sample, but to what degree is not clear; certainly the free water band at $\simeq$ 3250 cm^{-1} is no longer present, though a small amount of water strongly hydrogen-bonded to the acid could still be present. The resulting spectrum of the dehydrated acid at 10K is, however, much richer in well defined structure, with a correspondingly large increase in information content.

A search of the literature for the IR spectrum of anhydrously pure H_3PO_2 was negative, the only spectral data being that for aqueous solutions. In view of this deficiency, it was deemed worthwhile to obtain the spectrum of the deuterated species D_3PO_2 and attempt a vibrational assignment for the acid, using observed isotopic frequency shift data to aid in the analysis. The spectra of the aqueous and dehydrated D_3PO_2 aerosol at 10K are presented in Figure 5. The dehydrated spectra of H_3PO_2 and D_3PO_2, shown superimposed in Figure 6, show clearly the differences in the two spectra caused by the isotopic substitution.

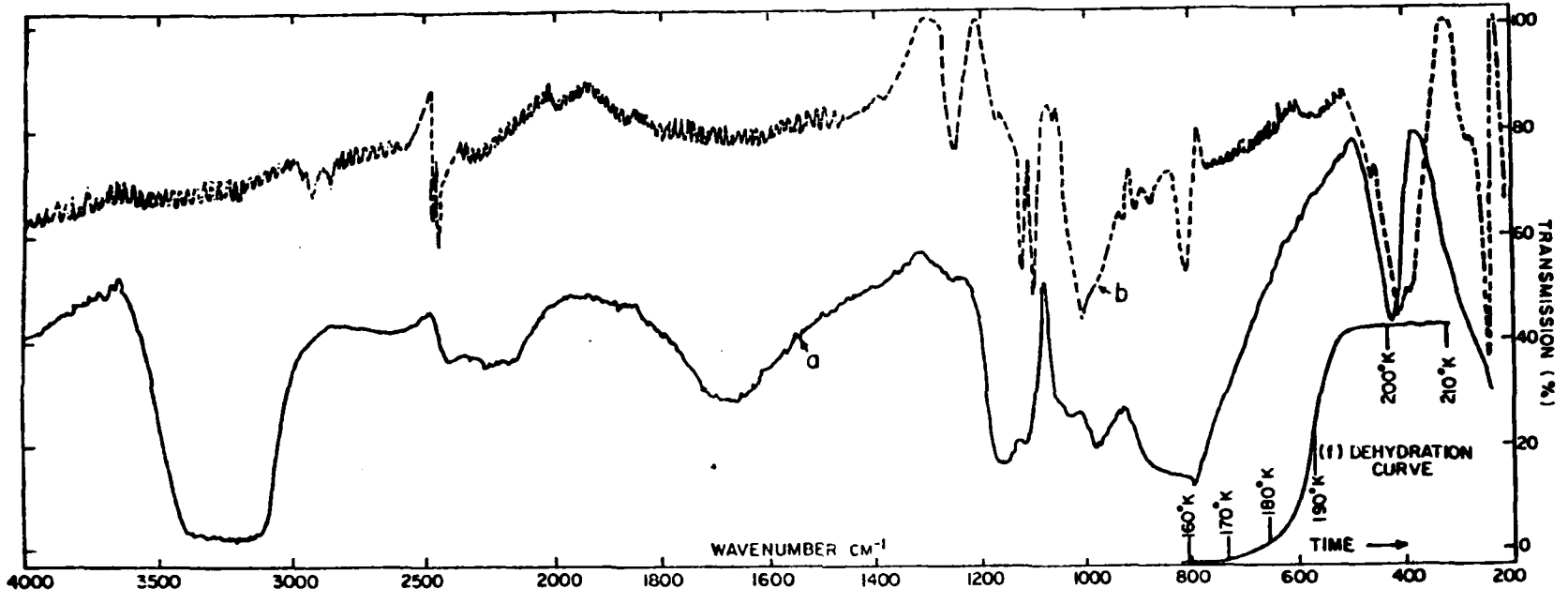

Figure 4. IR Spectra of Aqueous Hypophosphorous Acid Aerosol (≈90 wt%) Generated Using Helium Carrier Gas

(a) Aerosol as deposited at 10°K, (b) Aerosol after dehydration at 210°K and recorded at 10°K. The absorption feature showing at ≈250 cm^{-1} is an artifact due to a filter change in the spectrophotometer.

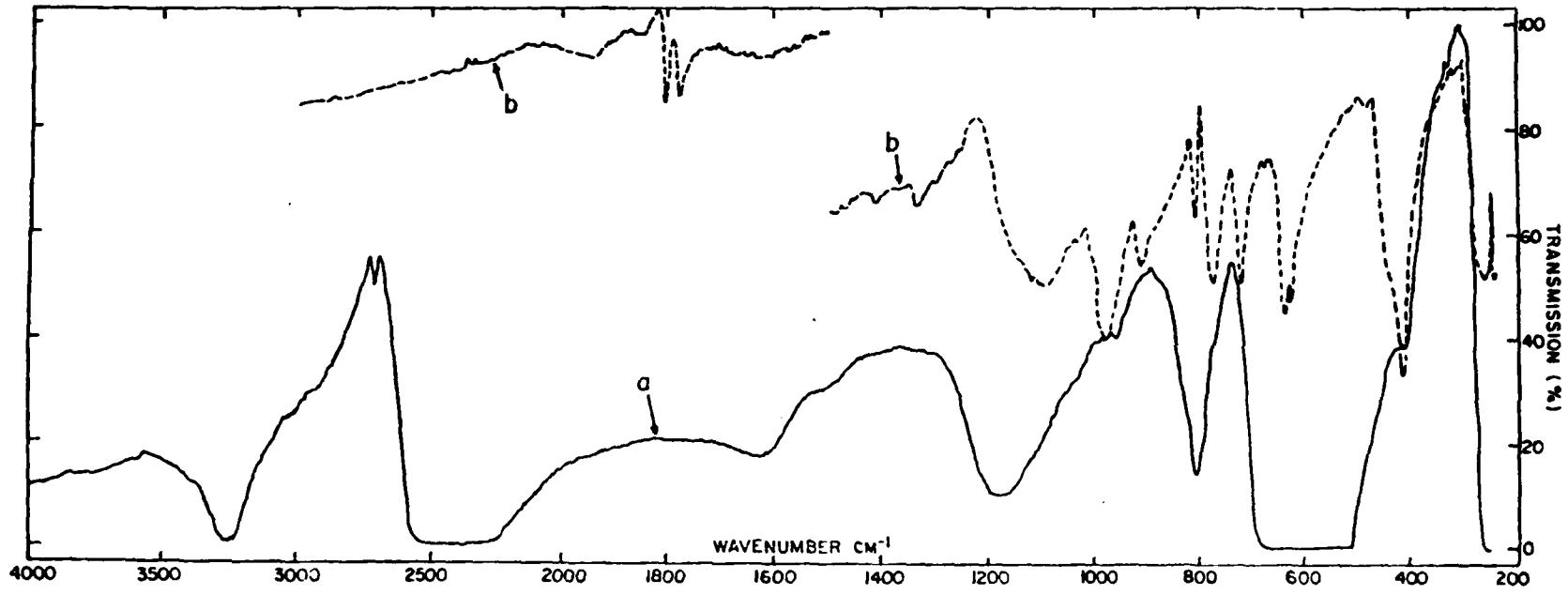

Figure 5. IR Spectra of Aqueous Deuterated Hypophosphorous Acid (≈50 wt%) Generated Using Helium Carrier Gas

(a) Aerosol as deposited at 10°K, (b) Aerosol after dehydration at 210°K, recorded at 10°K.

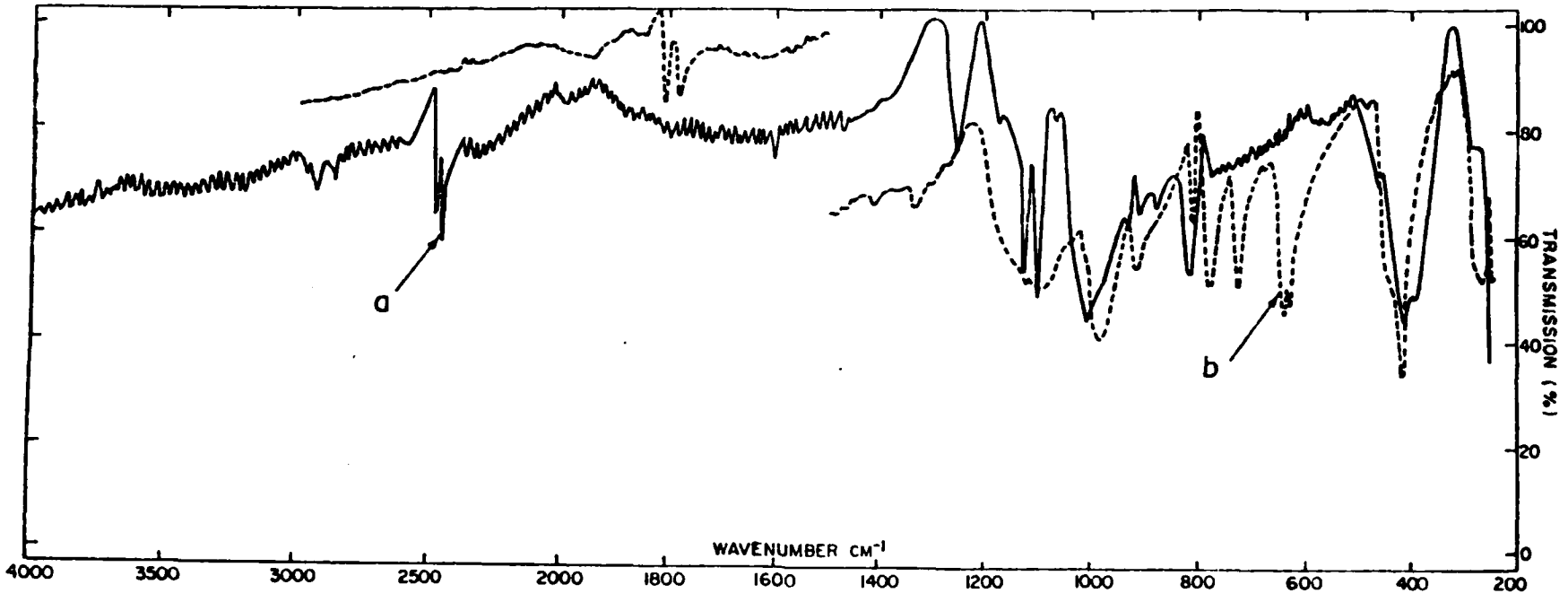

Figure 6. IR Spectra of Hypophosphorous Acid Aerosol, Generated Using Helium Carrier Gas Initially deposited at 10°K, dehydrated at 210°K and recooled to 10°K.

(a) H_3PO_2 and (b) D_3PO_2.

In order to make a vibrational assignment from the observed absorption bands of H_3PO_2 and D_3PO_2 recorded here, it is necessary to assume a molecular geometry since definitive data are not available in the literature. From the known chemical bonding characteristics of phosphorus and the monobasic character of the acid, the structure shown in Figure 7 is assumed for a gas phase molecule with free rotation of the OH group around the P-O axis. In the condensed phase, the effects of hydrogen bonding and crystal structure will almost certainly result in preferred orientations of the OH group with respect to the rest of the molecule. Two well-defined situations are possible: (1) the atoms O=P-O-H lie in the same plane, the latter bisecting the H-P-H angle, or (2) the H-atom lies outside the plane containing the O=P-O group. The two cases result in structures belonging to C_s and C_1 point groups, respectively. In either case 12 IR active frequencies are expected. For the former point group, the vibrations may be divided into two species: A', vibrations symmetric with respect to the plane of symmetry, and A", vibrations antisymmetric with respect to the plane of symmetry.

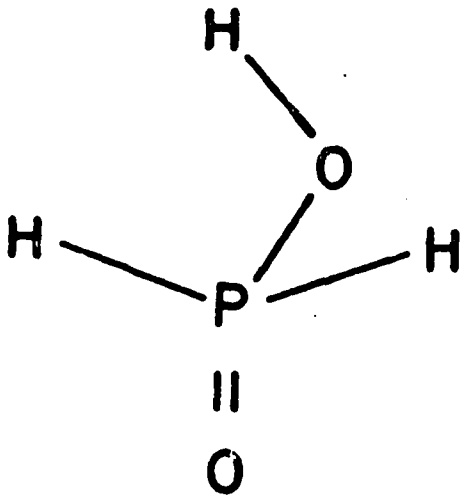

Figure 7. Structure of Hypophosphorus Acid Assuming C_s Symmetry

In the present case we have arbitrarily assumed C_s symmetry in deriving the tentative vibrational assignment shown in Table 1. Previous data on phosphorus acids,[16-19] some hypophosphorus acid salts,[20] and isotopic frequency shift measurements from the present study were used in arriving at the assignment. In hypophosphorous acid there are two P-H bonds which should result in two well-defined P-H stretching, modes of fairly similar frequency. Similar expectations apply to two lower frequency bending modes. In PH_3,[21] these frequencies lie in the 2300-2400 cm^{-1} and 980-1120 cm^{-1} regions for the stretching and bending modes, respectively. The four well-defined absorption bands at 2485, 2475, 1127, and 1103 cm^{-1} in the H_3PO_2 spectra are clearly assignable to PH stretching and bending modes. In D_3PO_2 the corresponding high frequency bands appear at 1805 and 1782 cm^{-1}.

Table 1. Vibrational Assignments and Frequencies of H_3PO_2 and D_3PO_2 Assuming C_s Symmetry

A' Symmetry Species				A" Symmetry Species		
Approximate mode description	H_3PO_2 cm^{-1}	D_3PO_2 cm^{-1}	H_3PO_2* cm^{-1}	Approximate mode description	H_3PO_2 cm^{-1}	D_3PO_2 cm^{-1}
O-H str	--	--	2650	PH_2 asym str	2485	1805
P-H_2 sym str	2475	1782	2410	PH_2 asym bend	1127	815
POH bend	1260	915	975	POH wag	914 880	640 630
				PO_2 wag	415	412
PH_2 sym bend	1103	790				
P-O str	~1100	~1100	1175			
P-O str	1010	980	975			
PO_2 bend	812	785				
PO_2 rock	780	722				

*Ref. 16 assignments from aqueous solution spectra

The higher frequency of the expected lower frequency doublet appears at 815 cm^{-1}, and it is likely that the second peak, expected at ≈ 790 cm^{-1}, overlaps with the broader feature at 785 cm^{-1}. The observed ratio $\nu(PH_2$ sym str.)/νPD_2 sym str.) at 1.39 agrees fortuitously well with the approximate calculated value based on the difference in isotopic masses of 1.39. Similarly, the ratio $\nu(PH_2$ asym str.) $\nu(PH_2$ asym bend)/$\nu(PD_2$ asym str.)$\nu(PD_2$ asym bend) observed at 1.90 again agrees fortuitously well with the approximate calculated value of 1.89. Absorption bands attributable to the O-H and O-D stretching modes, expected in the 2600-3000 cm^{-1} and 1800-2200 cm^{-1} regions, respectively, for the two acids were not observed. An absorption band at 1260 cm^{-1} (H_3PO_2) and the analogous feature at 915 cm^{-1} (D_3PO_2) are good candidates for the O-H and O-D bending modes; the observed ratio ν(POH bend)/ ν(POD bend) at 1.38 agrees well with the approximate calculated value of 1.39. Assignment of the out-of-plane POH bend (wag), which is expected to exhibit a marked isotope effect, is less certain; doublets at 914, 880 cm^{-1} (H_3PO_2), and at 640-630 cm^{-1} (D_3PO_2) are so assigned. The remaining P-O stretching and bending modes are assigned largely on the basis of previous literature values and the reasonableness of the assignment.

3.1.2 H_3PO_2 Phosphorous Acid.

Phosphorus acid was the second acid to be examined using the cryogenic sampling and temperature manipulating porcedures. Typical spectra are presented in Figures 8 and 9 for two concentrations of phosphorous acid aerosols (≈ 70 and ≈ 97 wt%) as deposited at 10K using helium carrier gas. As with the hypophosphorous spectra, in the more dilute solution, the spectrum of water is dominant and becomes much diminished at higher concentrations. Again, the dehydration procedure brings about a dramatic improvement in spectral detail. Also shown in Figure 8 are the spectra of the dehydrated sample, first recorded at 150K (curve b) and then at 10K (curve c). The improved spectral resolution brought about by lowering the temperature of the sample is obvious. No attempt was made to interpret this spectrum.

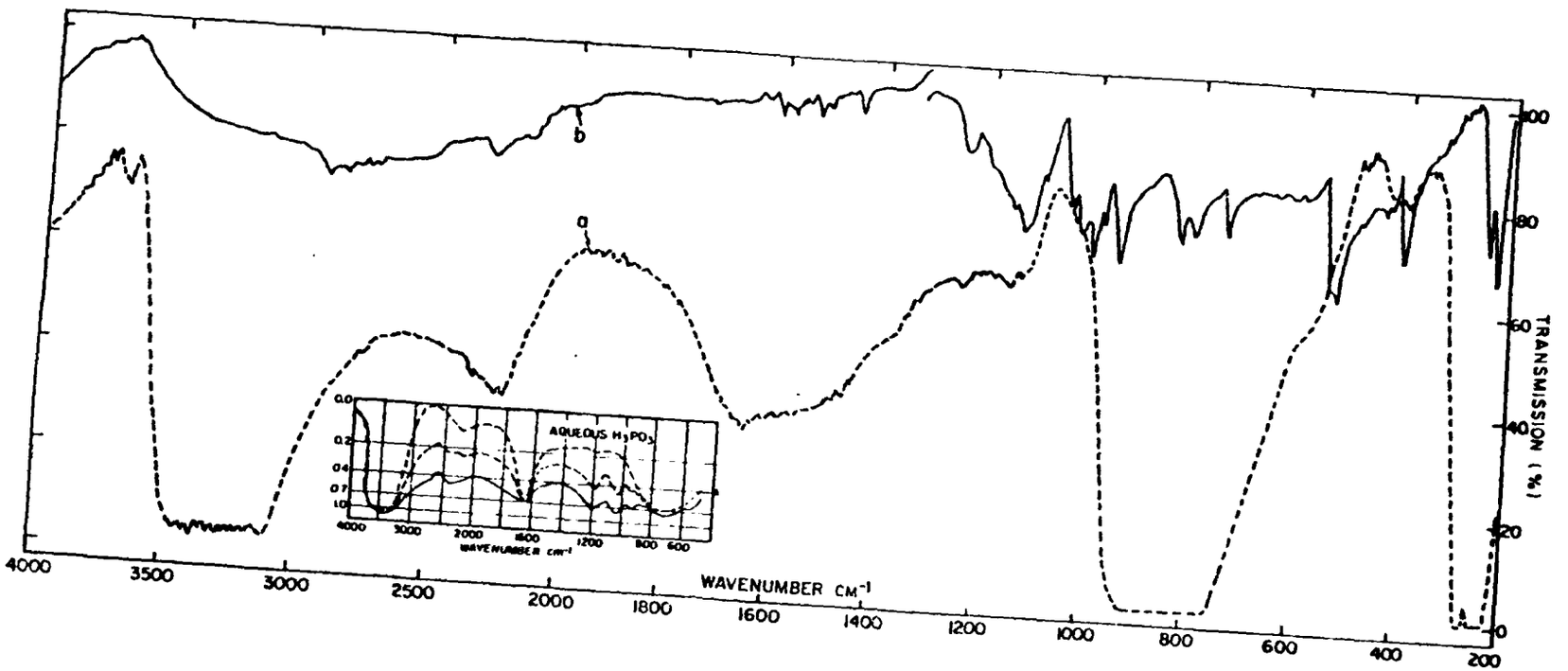

Figure 8. *IR Spectra of Aqueous Phosphorous Acid (≈70 wt%) Generated Using Helium Carrier Gas*

(a) As deposited and recorded at 10°K, (b) dehydrated at 200°K, recorded at 10°K. (The features at 2800-3000 cm^{-1} and 1400-1600 cm^{-1} are window impurity absorption bands.)

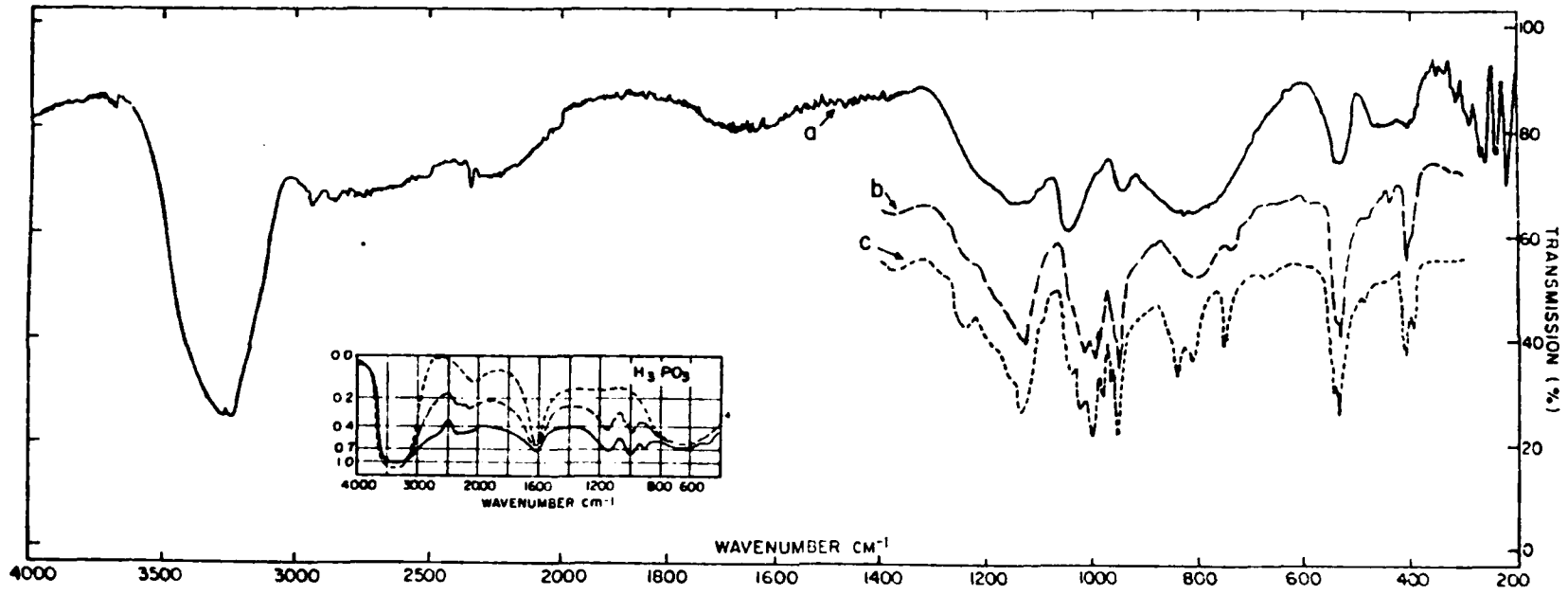

Figure 9. IR Spectra of Aqueous Phosphorous Acid (~97 wt%) Aerosol Generated Using Helium Carrier Gas

(a) As deposited and recorded at 10°K, (b) dehydrated at 220°K, recorded at 150°K, and (c) dehydrated at 220°K, recorded at 10°K.

3.1.3 H_3PO_4 - Phosphoric Acid.

The cryogenic spectra of a phosphoric acid aerosol before and after dehydration are presented in Figure 10. Unfortunately, in this case, the dehydration procedure did not result in as marked an improvement in spectral information content as it did with the previous two acids. There are several possible reasons for this:

(a) Increased hydrogen-bonding opportunities due to the larger number of OH groups in the molecule with concomitant absorption band broadening,

(b) Greater overlapping of absorption bonds due to the larger number of IR active frequencies,

(c) Increased absorption band broadening due to the presence in the sample of water that was not removed by the dehydration procedure.

Improved dehydration of the sample (case 3) could probably be achieved by modifying the window block heating and dehydration procedure. Due to limited funds, a modified dehydration approach was not tried since it would have required a fairly substantial modification of the equipment. At the present time, it is not certain which, or if all, of the above, is responsible for the decreased spectral resolution.

3.1.4 Pryophosphoric, Polyphosphoric and Meta Phosphoric Acids.

The spectra of these acids (and mixtures) are presented in Figures 11, 12, and 13, respectively. In general, these spectra all show a lack of much detailed structure on dehydration, similar to that observed with phosphoric acid. Almost certainly the reasons noted above for phosphoric acid are responsible. In addition, for the meta and polyphosphoric acids, the presence of several acids in the mixtures undoubtedly results in increased absorption band overlapping.

3.2 Phosphorus Acid Reference Spectra - In an Air Matrix.

As noted in the introduction to the previous section, air was initially used as a carrier gas when generating the cryogenic reference spectra for the phosphorus acids, but it was replaced for convenience with helium. Indeed all of

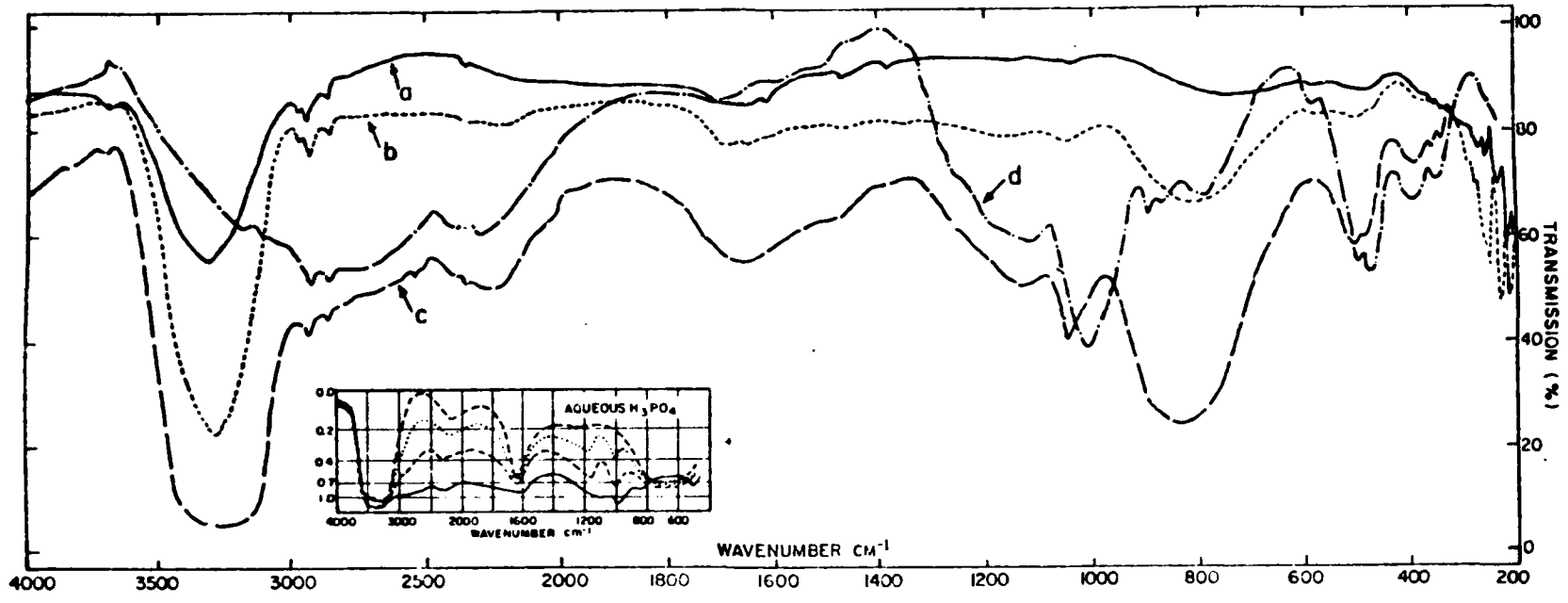

Figure 10. IR Spectra of Aqueous Phosphoric Acid (≈94 wt%) Generated Using Helium Carrier Gas

Curves (a), (b) and (c), successively heavier deposits at 10°K, recorded at 10°K, and (d) dehydrated at 220°K, recorded at 10°K. (The absorption features at 2800-3000 cm^{-1} are window impurity absorption bands.)

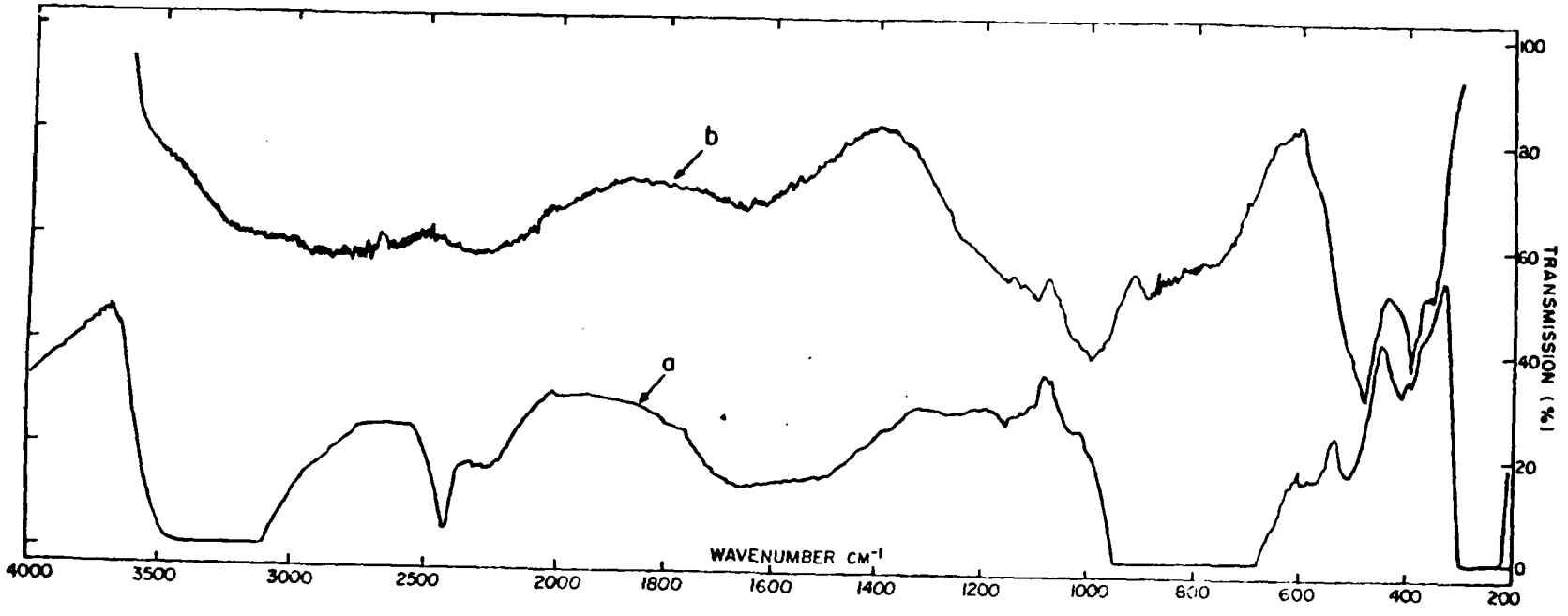

Figure 11. IR Spectra of Aqueous Pyrophosphoric Acid (≈54 wt%) Aerosol Generated Using Helium Carrier Gas

(a) As deposited and recorded at 10°K, (b) dehydrated at 230°K and recorded at 10°K.

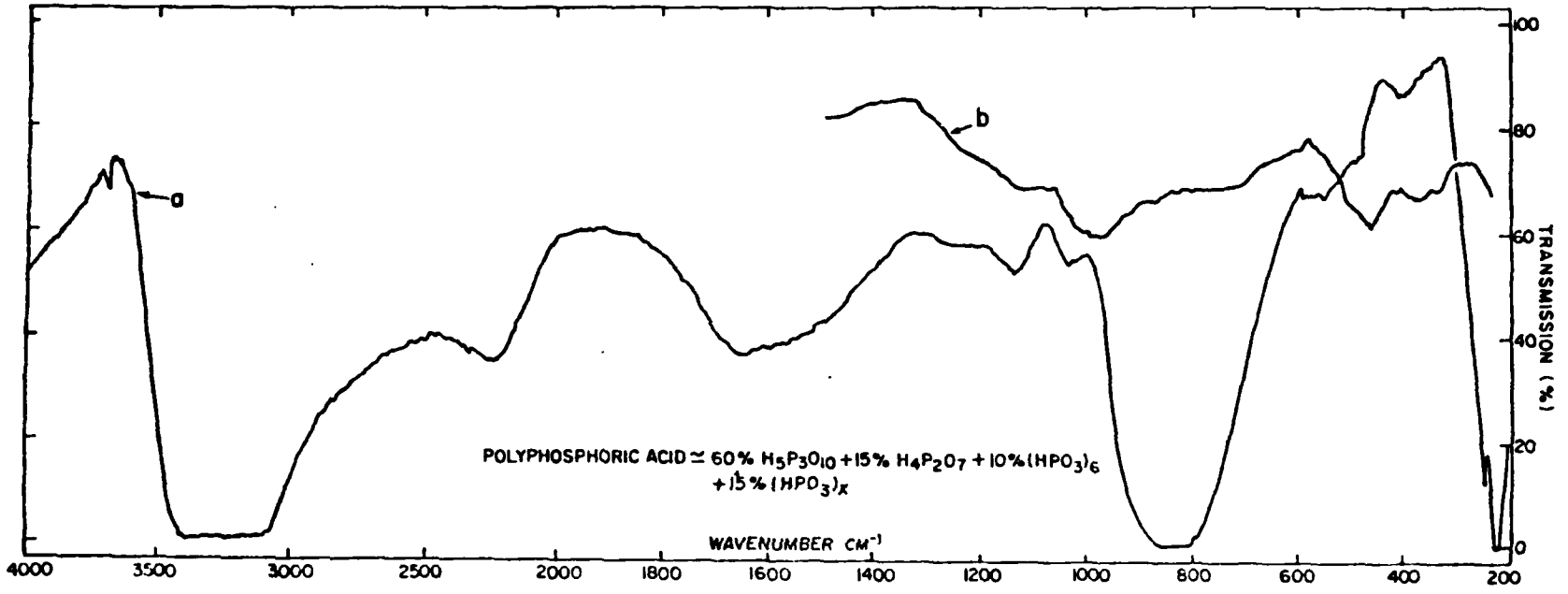

Figure 12. IR Spectra of Aqueous Polyphosphoric Acid (≃75 wt%) Aerosol Generated Using Helium Carrier Gas

(a) As deposited and recorded at 10°K, (b) Dehydrated at 220°K, recorded at 10°K.

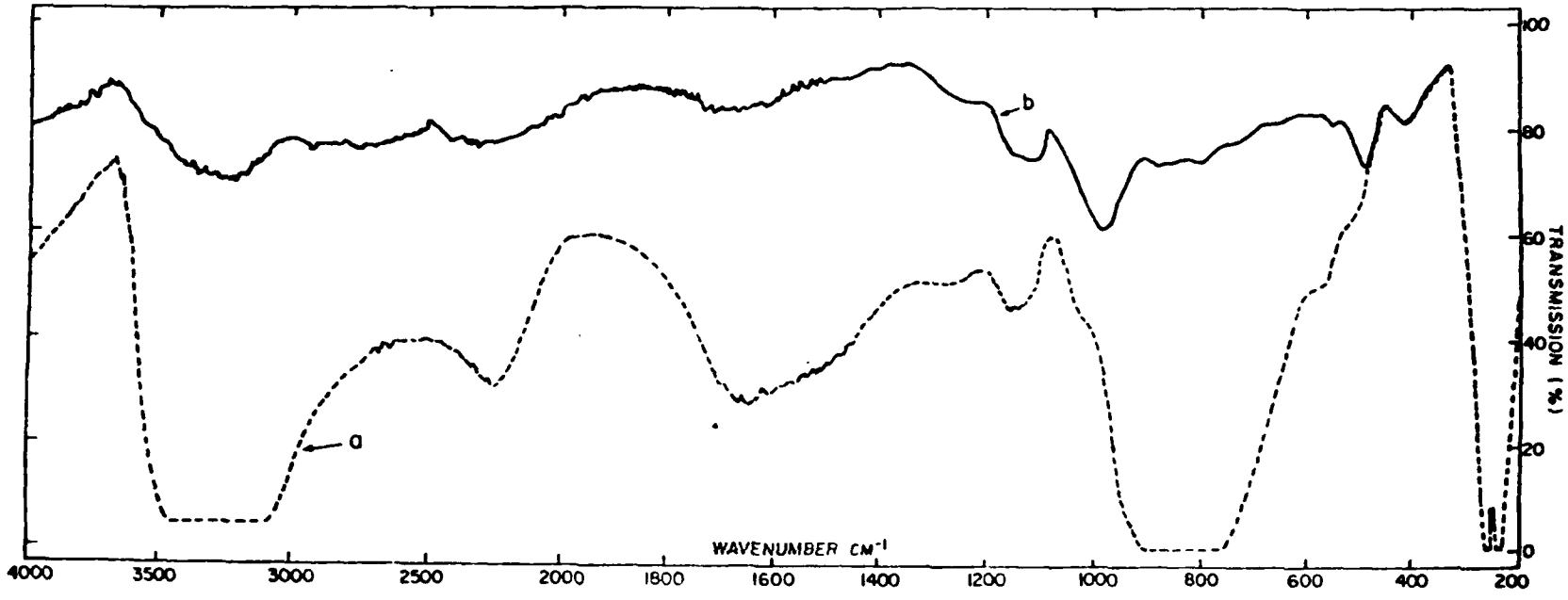

Figure 13. IR Spectra of Aqueous Metaphosphoric $(HPO_3)_n$ Acid (≃30 wt%) Aerosol Generated Using Helium Carrier Gas

(a) As deposited and recorded at 10°K, (b) dehydrated at 220°K, recorded at 10°K.

the reference spectra included in the report, thus far, were generated using helium as the carrier gas. Spectra, however, were obtained using air as the carrier gas for most of the phosphorus acids. In general, the information content of the spectra obtained by trapping the aerosol in an air matrix was somewhat inferior to that obtained in the absence of the air matrix. A typical example of spectra so obtained for a phosphoric acid aerosol is shown in Figure 14. In recording the spectrum denoted by curve (a), no attenuation of the IR spectrometer's reference beam was used to increase the apparent light transmission of the sample. The steady increase in transparency in traversing the 4000 to 200 cm^{-1} region, an effect commonly observed in matrix isolation spectroscopy, is usually and reasonably attributed to the light scattering effects of small crystalites of air formed during the condensation process. The quality of these spectra can be much improved by using reference beam attenuation. Curve b (Figure 14) shows the spectrum after removing the frozen air and curve c, the spectrum of the dehydrated phosphoric acid aerosol. In general, the aerosol plus air spectra provided no data of value not already present in the helium-generated aerosol spectra; hence, no other examples will be presented.

3.3 Spectral Obtained of Aerosol Generated by Burning Red or White Phosphorus in Air.

Several experiments were made in which both red and white phosphorus were burned in air at ≈ 50% relative humidity. Residence times in the reactor prior to trapping were varied from 1.2 to 120 sec. The aerosol was collected with the cryostat window block at 70K, to avoid condensing air on the window. Spectra were then obtained of the original collected material at 10K and after dehydration at 210K.

A typical spectrum, using burning red phosphorus as the aerosol source, is presented in Figure 15. A careful comparison of this and other spectra, with those obtained for the pure reference phosphorus acids, clearly showed that, although there were general similarities in the form of the spectra, a simple one-to-one correspondence with any one of the reference spectra did not exist. Qualitatively, aerosol spectra derived from the burning phosphorus showed most similarity to the phosphoric, polyphosphoric, and meta phosphoric acid spectra, an observation not at odds with recent findings[22] on the composition of the phosphorus smoke aerosol. An examination of the spectra of the aerosol obtained by

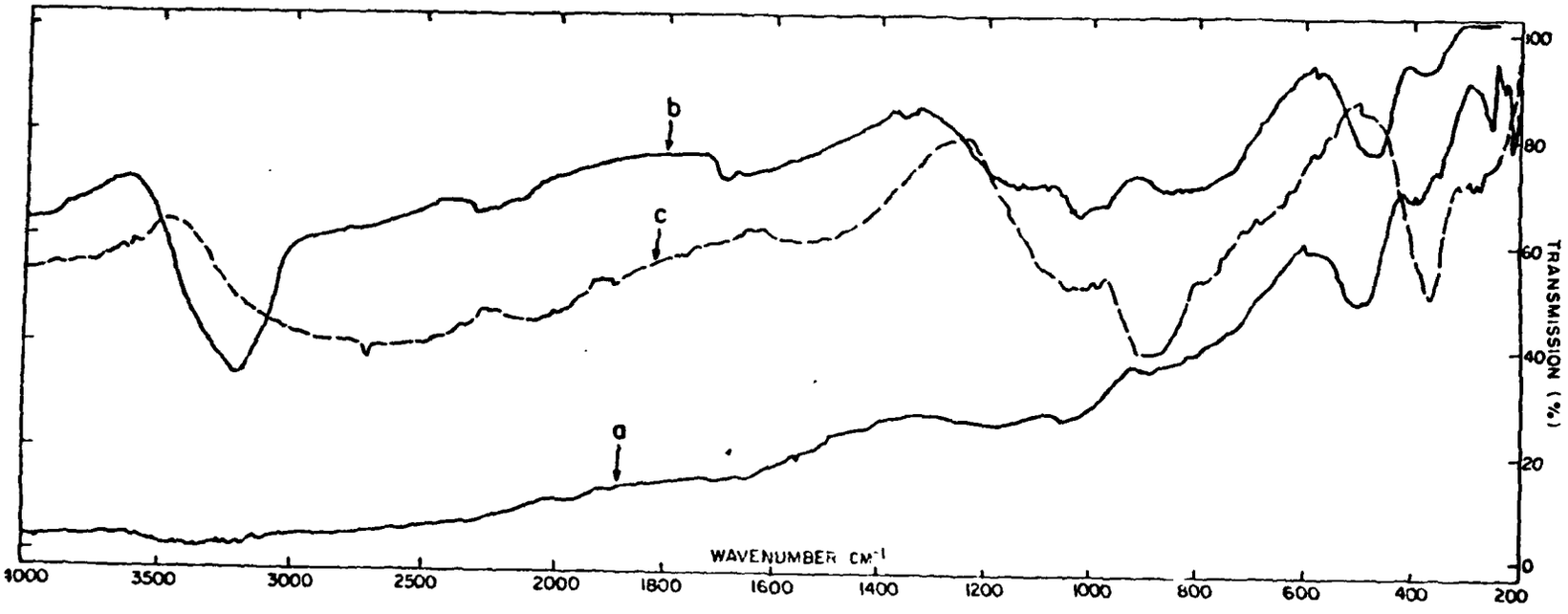

Figure 14. IR Spectra of Aqueous Phosphoric Acid (≈80 wt%) Aerosol Generated Using Zero Air Carrier Gas

(a) As deposited and recorded at 10°K, (b) After air removal at 60°K, recorded at 10°K, and (c) Dehydrated at 220°K, recorded at 10°K with abscissa expansion 2X.

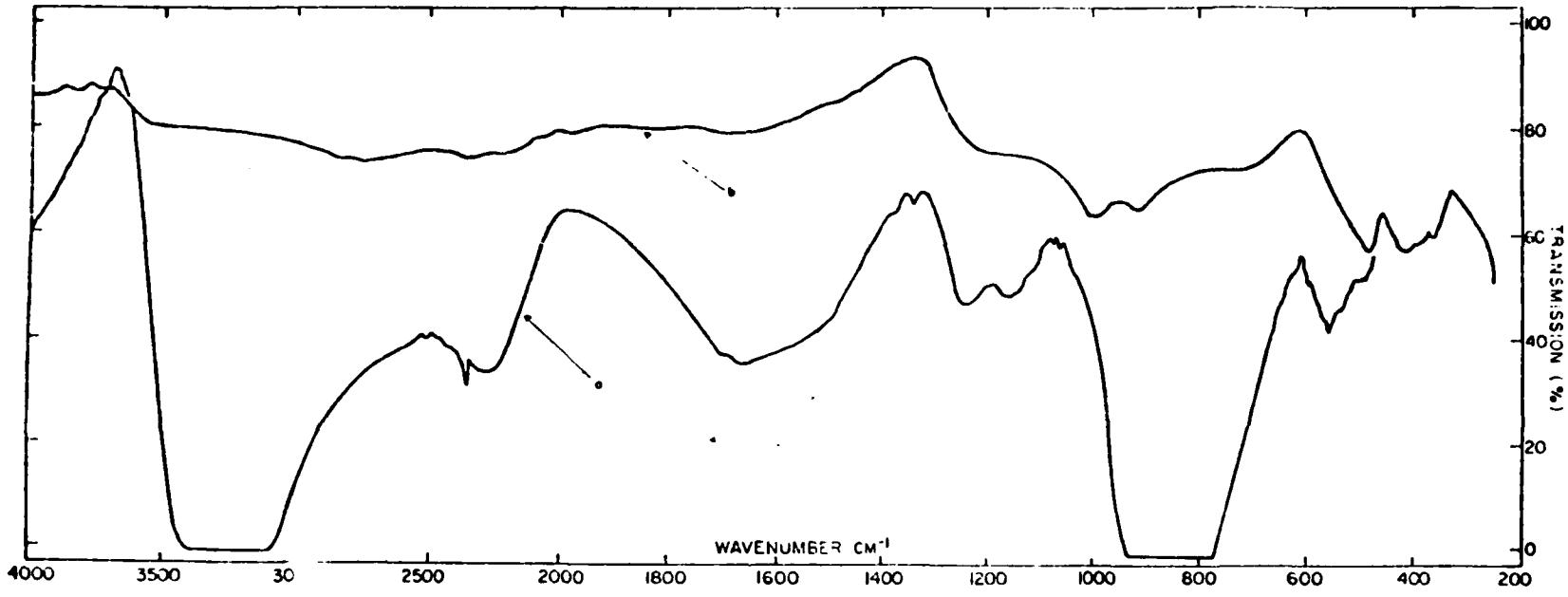

Figure 15. IR Spectra of Aerosol Formed by Burning Red Phosphorus in Zero Air (Relative Humidity ≃50%) Residence Time 120 sec

(a) As deposited at 70°K, spectra recorded at 10°K, and (b) after dehydration at 200°K, recorded at 10°K.

burning phosphorus indicates that the absorption band shoulder reaching a maximum at ≈ 1200 cm^{-1} had a greater intensity with respect to the absorption band maxima at ≈ 1000 cm^{-1} than in any of the phosphorus acid spectra noted above. This shoulder was also quite flat in the 1200-1050 cm^{-1} range, a shape which does not appear to be attainable by combining the various phosphorus acid reference spectra in any way, indicating the presence of some species for which reference spectra were not obtained.

In a slightly different approach, a few experiments were made to study the effects of relative humidity and reactor residence time on the hydrolysis of the phosphorus derived aerosol. Initially, red phosphorus was burned in zero air ($H_2O \leq 4$ ppm(v)), and the resultant aerosol cryogenically sampled. The IR spectrum of the trapped material is shown in Figure 16. A number of well-defined peaks were present, the frequencies of which are recorded in Table 2.

Table 2. Vibrational Frequencies of a P_2O_5 Formed by Burning Red Phosphorus in Zero Air Trapped in an Air Matrix at 10K

Observed Frequencies cm^{-1}	Literature Values[23] cm^{-1}
1416	1390
1400	
1025	1010
766	760
771	
571	573
421	424
412	
291	
281	278
271	

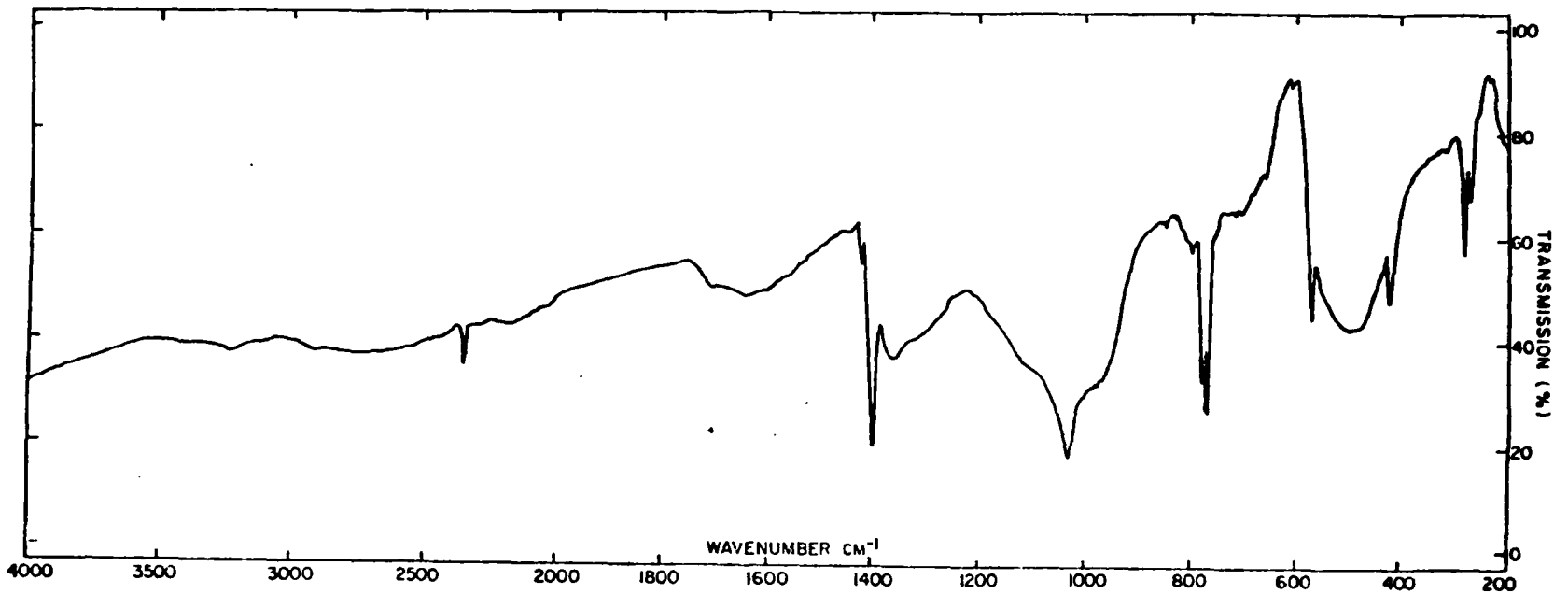

Figure 16. IR Spectrum of Aerosol Formed from Red Phosphorus Burned in Zero Air (H_2O < 4 ppm(v))

Deposited and recorded at 10°K. The peak at ≈2340 cm^{-1} is due to CO_2 in purity in the carrier gas.

For comparison purposes, literature[23] values are presented for the six IR-active vibration frequencies of P_2O_5 (six IR frequencies are expected assuming the molecule belongs to the T_d point group). In this latter study (the only one reported in the literature), the IR spectra were obtained using a slurry of P_2O_5 in nujol. No spectra of P_2O_5 were shown in the paper, and it is not known if the spectrum had the same general features as that reported here, i.e., six fairly sharp absorption maxima superimposed on several underlying broad absorption features. Assuming the aerosol is pure P_2O_5, the broad underlying features in the spectrum would not be expected, particularly at 10K. A possible cause of the spectral broadening might be associated with partial hydrolysis of the P_2O_5. Although the zero air used in the experiment air had a very low level of contained water vapor, it is possible that water adsorbed on the surfaces of the reactor and transfer lines may have been sufficient to cause some partial hydrolysis of the P_2O_5, which could result in spectral band broadening due to hydrogen bonding effects.

Some effects of varying reactor residence times and carrier gas humidities on the spectra of the aerosol formed by burning red phosphorus are shown in Figure 17. Spectral curve (a), for an aerosol formed with air at 5%-10% relative humidity and a reactor residence time of 10 sec, clearly shows the presence of sharp absorption bands due to P_2O_5. In addition, a more intense, broad underlying structure is present than that found in the "pure" P_2O_5 spectrum (Figure 16), and a broad new maximum appears at about 1335 cm^{-1}. No free water vapor appears to be present, since an absorption band characteristic of water isolated in an air matrix is not present at about 3750 cm^{-1}.

The spectrum shown in curve (b) is that of an aerosol formed with air at 20%-25% relative humidity and with a reactor residence time of 10 sec. In this case, no absorption features attributable to P_2O_5 are found, only a rather broad absorption in the 1350 to 400 cm^{-1} range with few well-defined maxima. The absorption maximum found at $\simeq$ 1335 cm^{-1} in curve (a) is now shifted to about 1240 cm^{-1}. Some free water was present in the gas phase at the time of trapping, since a 3750 cm^{-1} absorption band is found in the spectrum.

Finally the spectrum shown in curve (c) is that of an aerosol formed with air at 20%-25% relative humidity and with a reactor residence time of 1.2 sec. As in curve (b), no free P_2O_5 absorption bands are present, only the broad absorption

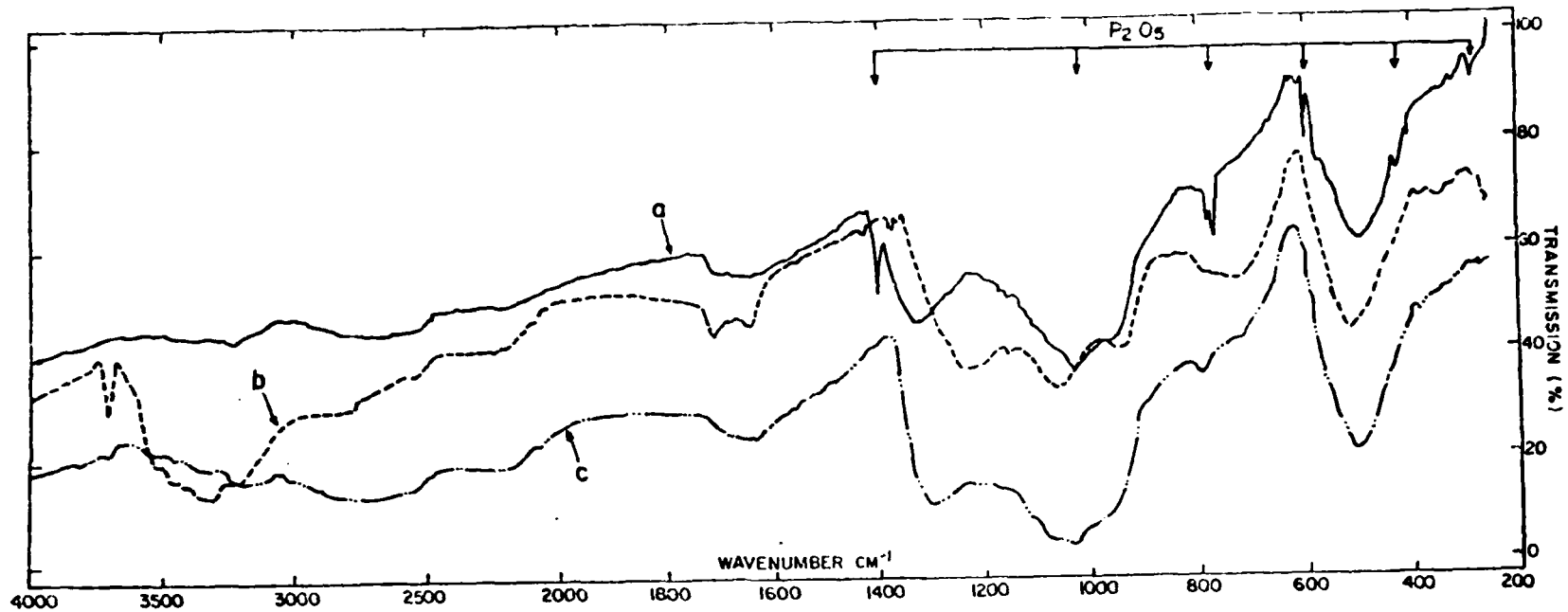

Figure 17. IR Spectra of Aerosol Formed by Burning Red Phosphorus in Air, Deposited and Recorded at 10°K

(a) Air relative humidity 5%-10% at 25°C, residence time in reactor, 10 sec, (b) Air relative humidity 20%-25%, residence time in reactor 10 sec, (c) Air relative humidity 20%-25%, residence time in reactor 1.2 sec. The arrows indicate absorption bands due to P_2O_5.

feature. This time, however, the absorption maximum occuring at 1335 cm^{-1} and 1240 cm^{-1} in curves (a) and (b), respectively, now appears at 1290 cm^{-1}. A weak absorption band characteristic of free water appears at ≈ 3750 cm^{-1}; however, it is less intense than that in curve (b). All things being equal, it might be expected that more free water would be present in the gas phase at the shorter, compared to the longer, residence time for the same initial relative humidity; whereas, the data show the reverse to be true. There are two factors that might account for the observed behavior: (1) at the higher gas flow rates required for the shorter reactor residence time, the bubbler used to saturate the gas flow may not have been efficient, and (2) the rate at which the phosphorus burned appeared to increase at the higher gas flow rates, increasing the demand on the available water.

The above data shows clearly that, when P_2O_5 undergoes hydrolysis, an absorption band starts to "grow in" which, as the extent of hydrolysis increases, moves, based on the present data, from 1335 → 1290 → 1240 cm^{-1}. It is interesting to note that in measurements on the extinction spectra of phosphorus smokes, an absorption maximum is found at about 1270 cm^{-1}, which decreases in intensity with both time and relative humidity. As has been noted, this maximum is not typical of any of the known lower polymers of the various phosphorus acids. It appears reasonable to conclude that the hydrolysis of burning phosphorus results initially in chemical species with large molecular weights of ill-defined structure. As the hydrolysis proceeds, recognizable structures of the higher polymeric phosphorus acids appear, which eventually are hydrolyzed to the lower acids.

From a chemical viewpoint, it is of some interest to consider the source of the broad absorption band (1335-1240 cm^{-1}) that starts to grow in on hydrolysis of the burning phosphorus aerosol. An obvious possibility is its assignment to an OH bending mode, which might be expected to lie in this region and shift to longer wavelengths as increased hydrogen bonding occurs. An alternative possibility would be to attribute the feature to a P=O stretching mode. In P_2O_5 the 1400 cm^{-1} absorption band corresponds to a P=O stretching mode. This frequency in the monomeric phosphorus acids appears to lie in the 1100-1200 cm^{-1} region. It is believed that hydrogen bonding to the oxygen of the P=O group does occur in the acids and is partially responsible for the effective weakening of the P=O bond,

resulting in the frequency dropping markedly from that in P_2O_5. If phosphorus were burned in air humidifed with deuterated water, a choice between the two possibilities noted above could probably be made.

REFERENCES

1. van der Hulst, H.C., Light Scattering of Small Particles, Wiley, 1957.

2. Kerker, M., The Scattering of Light and Other Elecgromagnetic Radiation, Academic Press, 1968.

3. Kohl, R.H. ARCSL-CR-81023. Proceedings of the 1979 Chemical Systems Laboratory Scientific Conference on Obscuration and Aerosol Research. December 1980. UNCLASSIFIED Report.

4. Kohl, R.H. ARCSL-SP-82021. Proceedings of the 1980 Chemical Systems Laboratory Scientific Conference on Obscuration and Aerosol Research. June 1983. UNCLASSIFIED Report.

5. Kohl, R.H. ARCSL-SP-82022. Proceedings of the 1981 Chemical Systems Laboratory Scientific Conference on Obscuration and Aerosol Research. June 1983. UNCLASSIFIED Report.

6. Kohl, R.H. ARCSL-SP-83011. Proceedings on the 1982 Chemical Systems Laboratory Scientific Conference on Obscuration and Aerosol Research. June 1983. UNCLASSIFIED Report.

7. Milham, M.E., Anderson, D.H., and Frickel, R.H., Applied Opitcs 21, 2501 (1982).

8. Technical Manual TM3-215 (AFM355-7). Military Chemistry and Chemical Agents. Departments of the Army (and Air Force). December 1963.

9. Engineering Design Handbook. AMCP 706-185. Military Pyrotechnic Series Part 1. US Army Material Command. April 1967.

10. Gillespie, E.R., and Johnstone, H.F., Particle Size Distribution in Some Hygroscopic Aerosols. Chemical Engineering Progress 51 (No. 2) (1955).

11. Carlon, H.R., Anderson, D.H., Milham, M.E., Tarnove, T.L., Frickel, R.H., and Sindoni, O.I. Infrared Extinction Spectra of Some Common Liquid Aerosols. Applied Optics 16 (No. 6) (1977).

12. Findelsten, L. CRDL Special Publication 1-42. History of Research and Development of the Chemical Warfare Service in World War II. Screening Smokes Part II, June 1964.

13. Tarnove, T.L. Studies on the Chemistry of the Formation of Phosphorus-Derived Smokes and Their Implication for Phosphorus Smoke Munitions. Chemical Systems Laboratory Technical Report ARCSL-TR-80049. October 1980.

14. Katz, S., Snelson, A., Butler, R., Bock, W., Rajendran, N., and Relwani, S., Physical and Chemical Characterization of Military Smokes. Part III. White Phosphorus - Felt Smokes. Final Report. Contract No. DAMD17-78-C-8085. Sponsored by US Army Medical Research and Development Command. Fort Detrick, MD. 1981.

15. Hallam, H.E., Ed. Vibrational Spectroscopy of Trapped Species. John Wiley Sons, New York, NY. 1973.

16. Leuchs, M., and Zundel, G., Can. J. Chem. 57, 487 (1979).

17. Detoni, S., and Hudzi, D. Spectrochimica Acta 20, 949 (1964).

18. Chapman, A.C., and Thirlwell, L.E. Ibid 20, 937 (1964).

19. Levene, R.J., Powell, D.B., and Steele, D. Ibid 22, 2033 (1966).

20. Tsubai, M. J. Amer. Chem. Soc. 79, 1351 (1957).

21. Stevenson, D.P. J. Chem. Phys. 8, 285 (1940).

22. Brazell, R.S., Moneyhun, J.H., and Holmberg, R.W. Paper presented at CSL 1983 Scientific Conference on Obscuration and Aerosol Research, Aberdeen Proving Grounds, MD.

23. Chapman, A.C. Spectrochimica Acta 24A, 1687 (1968).

APPENDIX

AEROSOL PARTICLE SIZE MEASUREMENTS ON SELECTED AQUEOUS PHOSPHORUS ACIDS GENERATED IN THE DE VILBIS NEBULIZER

A De Vibilis-40 nebulizer was used to generate acid aerosols. Each acid aerosol was drawn into the nebulizer with dilution air to observe particle size and concentration. For comparison reasons and to achieve the desired concentration, a nebulizer pressure of 0.3 inch water was maintained except in the case of $(HPO_3)_n$ acid, in which a nebulizer pressure of 1 inch water was used. For all cases, 20 liters/min of dry air was used for dilution. The aerosol dilution system is shown in Figure A-1. The aerosol generation and air dilution is continuous.

The aerosol sampling line is shown in Figure A-2. An important function of this system was the reduction of the aerosol concentration to a level suitable for measurement by the aerosol monitor. A dilution of 1000 (± 10):1 was used with a total transit time from sampling location to detector of somewhat less than 1 min. A feature of the system is the use of recirculated air for dilution to preserve the physical characteristics of the sample. The aerosol particles were analyzed using the instrument described below. The Particle Measuring Systems, Inc. Active Scattering Aerosol Spectrometer (ASAS), Model ASAS-300-PMT, was used for sizing particles within the size range of 0.088 to 3.00 μm. Particles passing through the laser cavity of a continuous He-Ne laser produce pulses of light proportional only to their size and position in the beam. A pair of photomultiplier detectors image the light impulses and select pulses produced by particles in the correct sample space. A pulse height analyzer then determines the particle sizes. The output of the ASAS is grouped into size classes as shown in Table B-1.

Experimental data are presented in the following Figures and Tables for the various phosphorus acids.

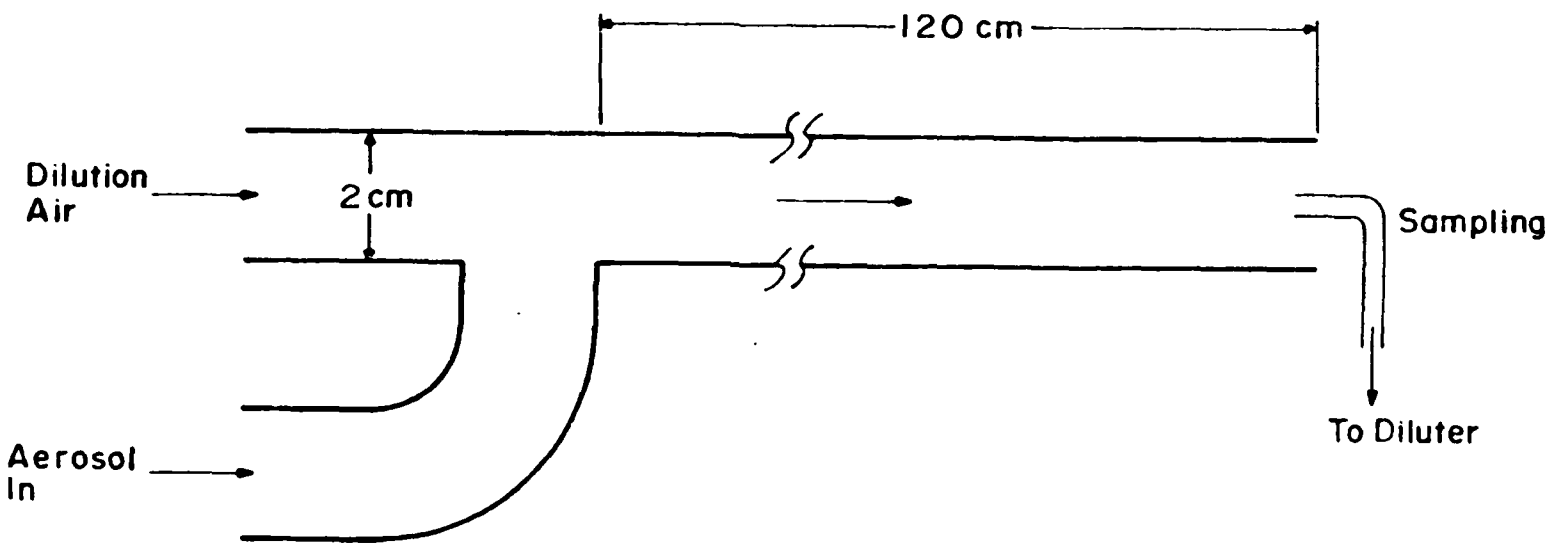

Figure A-1. Schematic Diagram of Acid Aerosol Dilution System

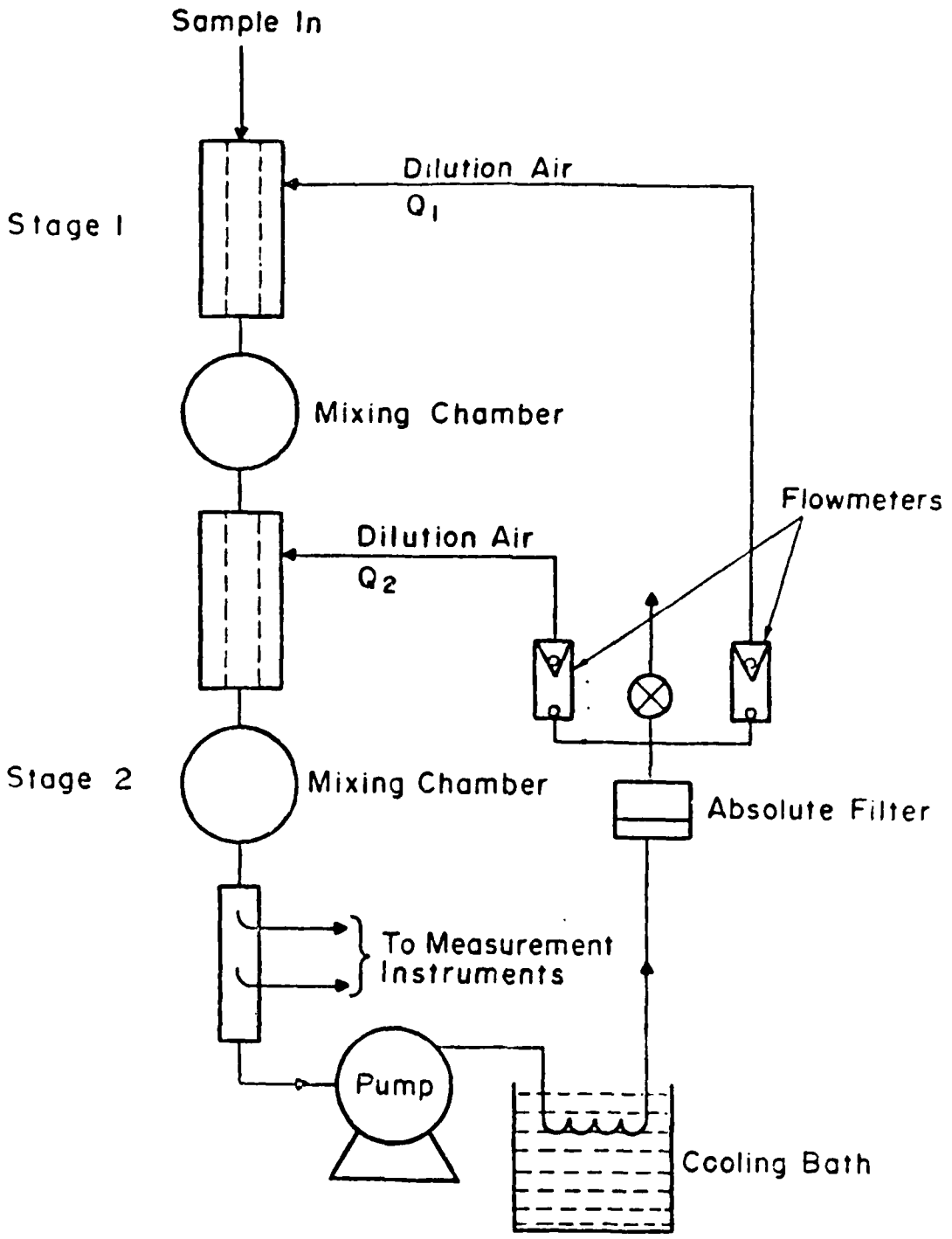

Figure A-2. Aerosol Sampling Line and Dilution System

Table B-1. ASAS Size Range Data

ASAS range	Channel	Size interval μm	Interval width μm	d_j Midrange diameter, μm
3	1-7	0.088-0.144	0.056	0.116
3	5-15	0.144-0.208	0.064	0.176
2	4-15	0.210-0.390	0.180	0.300
1	408	0.388-0.503	0.115	0.445
1	9-15	0.508-0.676	0.168	0.592
0	2	0.690-0.855	0.165	0.772
0	3	0.855-1.020	0.165	0.938
0	4	1.020-1.85	0.165	1.102
-	-	-	-	-
0	15	2.835-3.000	0.165	2.917

A summary of the analytical data is given in Table
cummulative plots for Experiments 1 and 2. The summary of data for each
experiment follows.

Table B-2. Calculated Number Mean Diameter of Acid Aerosol for Experiments #1 through #8

Experiment No.	Acid Type	Nebulizer Condition	Number Mean Dia (μm)	Dilution air flow (filter/min)
1	Sulfuric acid[(a)]	air n.p. = 0.3" water	0.51	20
2	Sulfuric acid	helium n.p. = 0.3" water	0.32	20
3	H_3PO_4, 53.3% wt	air n.p. = 3" water	0.51	20
4	H_3PO_4, 85% wt	air n.p. = 0.3" water	0.48	20
5	H_3PO_2, 50% wt	air n.p. = 0.3" water	0.45	20
6	H_xPO_4, 78.2%	air n.p. = 0.3" water	0.56	20
7	H_3PO_3, 70.9%	air n.p. = 3" water	0.40	20
8	$(HPO_3)_n$, 43.3%	air n.p. = 1" water	0.41	20

(a) Data was obtained for H_2SO_4 to test the equipment prior to experiments with the phosphorus acids.

n.p. = nominal pressure

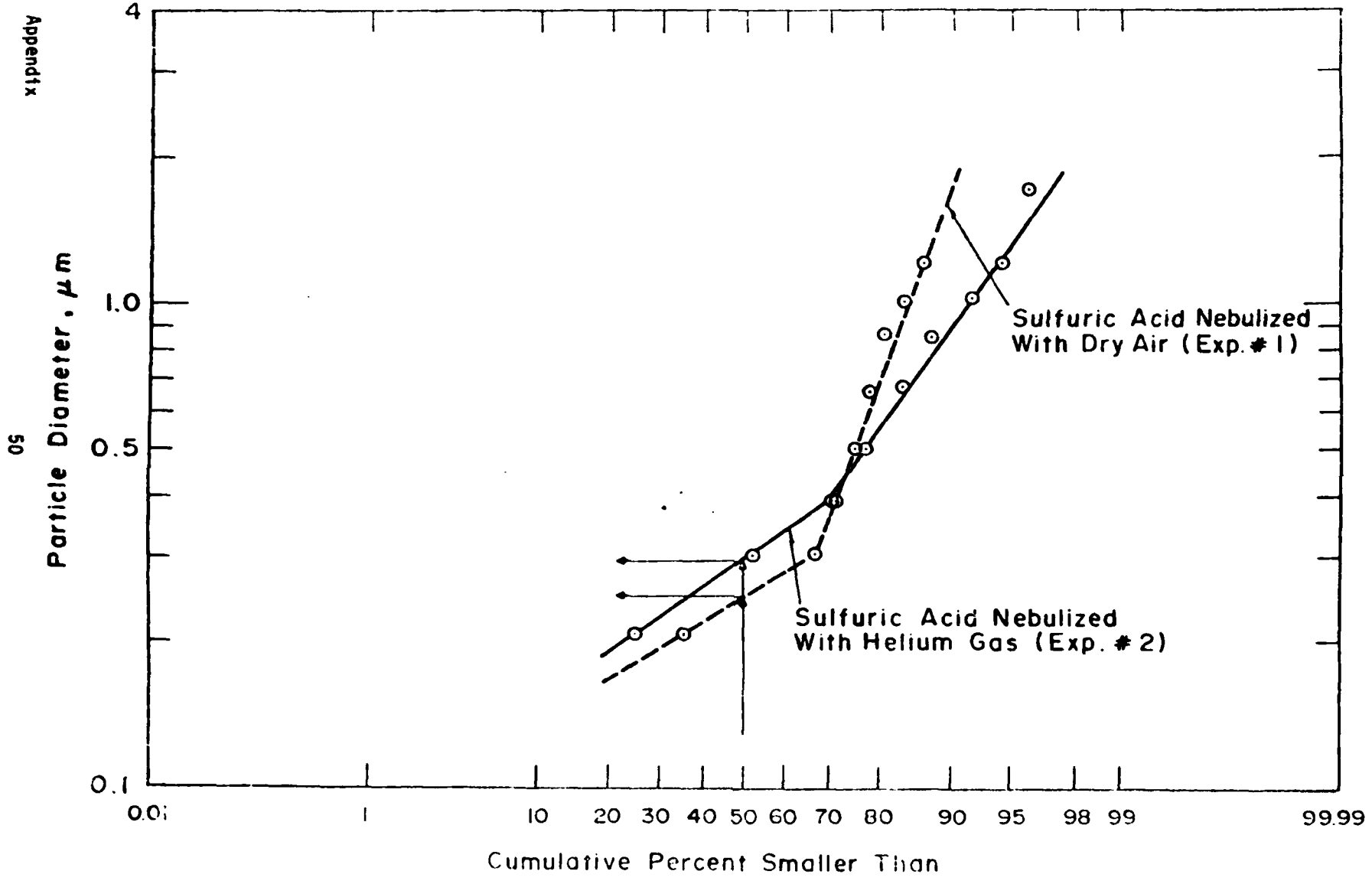

Figure A-3. Log Probability Plots for Experiments No. 1 and No. 2

Experiment #1

Particle Size Data for H_2SO_4, Air Carrier Gas

Particle dia. µm	Number of Particles	Fraction %	Cummulative %
	6	0.17	99.84
2.918	7	0.20	99.64
2.753	10	0.29	99.35
2.588	3	0.09	99.26
2.423	6	0.17	99.09
2.258	11	0.32	98.77
2.093	6	0.17	98.60
1.928	20	0.58	98.02
1.763	70	2.03	95.99
1.598	166	4.81	91.18
1.432	175	5.07	86.11
1.270	167	4.83	81.28
1.102	131	3.79	77.49
0.938	129	3.73	73.76
0.773	107	3.10	70.66
0.592	164	4.75	65.91
0.448	157	4.55	61.36
0.300	291	8.43	52.93
0.176	566	16.39	36.54
0.116	1267	36.54	-
AF	-	-	-
Total	3454		

Appendix

Experiment #2

Particle Size Data for H_2PO_4, Helium Carrier Gas

Particle dia. µm	Number of Particles	Fraction %	Cummulative %
	-	-	
2.918	-	-	
2.753	-	-	
2.588	-	-	
2.423	-	-	
2.258	-	-	100.00
2.093	1	.325	99.68
1.928	1	.325	99.35
1.763	-	-	99.35
1.598	-	-	99.35
1.432	7	2.28	97.07
1.270	8	2.61	94.46
1.102	7	2.28	92.18
0.938	14	4.56	87.62
0.773	12	3.91	83.71
0.592	19	6.19	77.52
0.448	23	7.49	70.03
0.300	55	17.92	52.11
0.176	82	26.71	25.40
0.116	78	25.4	-
AF	-	-	-
Total	307		

Appendix

Experiment #3

Particle Size Data for H_3PO_4 (53.3 Wt. %) Air Carrier Gas

Particle dia. μm	Number of Particles	Fraction %	Cumulative %
	9	0.39	99.62
2.918	6	0.26	99.36
2.753	9	0.39	98.97
2.588	3	0.13	98.84
2.423	11	0.48	98.36
2.258	6	0.26	98.10
2.093	5	0.22	97.88
1.928	7	0.30	97.58
1.763	5	0.22	97.36
1.598	30	1.30	96.06
1.432	104	4.51	91.55
1.270	143	6.20	85.35
1.102	116	5.03	80.32
0.938	112	4.85	75.47
0.773	71	3.08	72.39
0.592	123	5.33	67.06
0.448	134	5.81	61.25
0.300	234	10.14	51.11
0.176	316	13.70	37.41
0.116	863	37.41	-
AF	-	-	-
Total	2307		

Experiment #4

Particle Size Data for H_3PO_4 (85 Wt. %) Air Carrier Gas

Particle dia. µm	Number of Particles	Fraction %	Cummulative %
	2	0.15	99.85
2.918	2	0.15	99.70
2.753	4	0.29	99.41
2.588	5	0.37	99.04
2.423	3	0.22	98.82
2.258	1	0.07	98.75
2.093	3	0.22	98.53
1.928	3	0.22	98.31
1.763	5	0.37	97.94
1.598	7	0.51	97.43
1.432	64	4.68	92.75
1.270	100	7.31	85.44
1.102	80	5.85	79.59
0.938	90	6.58	73.01
0.773	47	3.43	69.58
0.592	82	5.99	63.59
0.448	88	6.43	57.16
0.300	115	8.41	48.75
0.176	169	12.35	36.40
0.116	498	36.40	-
AF	-	-	-
Total	1368		

Experiment #5

Particle Size Data for H_3PO_2 (50 Wt. %) Air Carrier Gas

Particle dia. µm	Number of Particles	Fraction %	Cummulative %
	11	0.27	99.74
2.918	9	0.22	99.52
2.753	11	0.27	99.25
2.588	8	0.19	99.06
2.423	12	0.29	98.77
2.258	12	0.29	98.48
2.093	9	0.22	98.26
1.928	10	0.24	98.02
1.763	4	0.10	97.92
1.598	14	0.34	97.58
1.432	148	3.58	94.00
1.270	235	5.68	88.32
1.102	203	4.91	83.41
0.938	198	4.79	78.62
0.773	139	3.36	75.26
0.592	221	5.34	69.92
0.448	260	6.29	63.63
0.300	327	7.91	55.72
0.176	718	17.36	38.36
0.116	1586	38.36	-
AF	-	-	-
Total	4135		

Experiment #6

Particle Size Data for H_xPO_4 (78 Wt. %) Air Carrier Gas

Particle dia. μm	Number of Particles	Fraction %	Cummulative %
	2	0.19	99.81
2.918	-	-	99.81
2.753	3	0.29	99.52
2.588	3	0.29	99.23
2.423	5	0.48	98.75
2.258	4	0.38	98.37
2.093	3	0.29	98.08
1.928	2	0.19	97.89
1.763	3	0.29	97.60
1.598	12	1.15	96.45
1.432	63	6.04	90.41
1.270	100	9.59	80.82
1.102	72	6.90	73.92
0.938	79	7.57	66.35
0.773	50	4.79	61.56
0.592	76	7.29	54.27
0.448	63	6.04	48.23
0.300	98	9.40	38.83
0.176	97	9.30	29.53
0.116	308	29.53	-
AF	-	-	
Total	1043		

Experiment #7

Particle Size Data for H_3PO_3 (70.9 Wt. %) Air Carrier Gas

Particle dia. µm	Number of Particles	Fraction %	Cummulative %
	18	0.22	99.77
2.918	11	0.13	99.64
2.753	17	0.21	99.43
2.588	21	0.26	99.17
2.423	19	0.23	98.94
2.258	9	0.11	98.83
2.093	13	0.16	98.67
1.928	15	0.18	98.49
1.763	14	0.17	98.32
1.598	118	1.44	96.88
1.432	279	3.41	93.47
1.270	328	4.01	89.46
1.102	275	3.36	86.10
0.938	288	3.52	82.58
0.773	169	2.07	80.51
0.592	284	3.47	77.04
0.448	275	3.36	73.68
0.300	451	5.51	68.17
0.176	3187	38.97	29.20
0.116	2388	29.20	-
AF	-	-	-
Total	8179		

Experiment #8

Particle Size Data for $(HPO_3)n$ (43.3 Wt. %) Air Carrier Gas

Particle dia. µm	Number of Particles	Fraction %	Cummulative %
	-	-	
2.918	1	0.34	99.69
2.753	1	0.34	99.35
2.588	-	-	99.35
2.423	-	-	99.35
2.258	-	-	99.35
2.093	2	0.68	98.67
1.928	-	-	98.67
1.763	1	0.34	98.33
1.598	1	0.34	97.99
1.432	2	0.68	97.31
1.270	9	3.04	94.27
1.102	15	5.07	89.20
0.938	27	9.12	80.08
0.773	20	6.76	73.32
0.592	34	11.49	61.83
0.448	39	13.18	48.65
0.300	33	11.15	37.50
0.176	54	18.24	19.26
0.116	57	19.26	-
AF	-	-	-
Total	296		

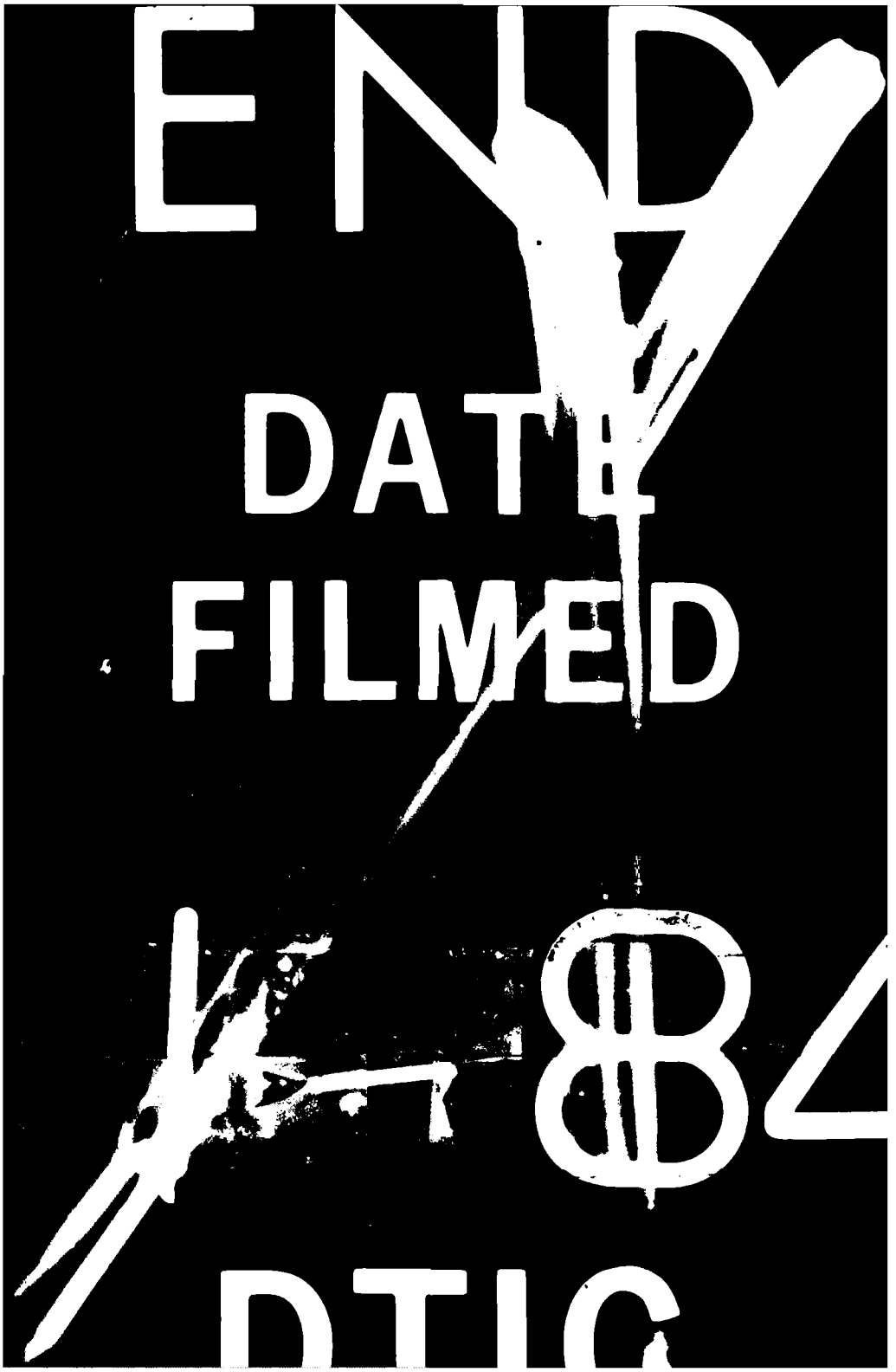
END
DATE
FILMED
84
DTIC

AD-A146 188 AN INVESTIGATION OF A CRYOGENIC MATRIX ISOLATION APPROACH FOR CHARACTERIZ..(U) IIT RESEARCH INST CHICAGO IL A SNELSON JUL 84 CRDC-CR-84050 DAAK11-81-K-0007 2/2

UNCLASSIFIED F/G 7/4 NL

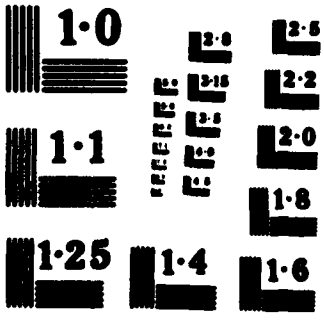
1·0
1·1
1·25
1·4
1·6
1·8
2·0
2·2
2·5

SUPPLEMENTARY

INFORMATION

AD-A146188

DEPARTMENT OF THE ARMY
Chemical Research and Development Center
Headquarters, US Army Armament, Munitions and Chemical Command
Aberdeen Proving Ground, Maryland 21010-5423

ERRATUM SHEET

Report No. CRDC-CR-84050

Title: An Investigation of a Cryogenic Matrix Isoslation Approach for Characterizing Phosphorus Acid Aerosol. Final Report on IITRI Contract No. C06540

Author: Alan Snelson, IIT Research Institute

Date: July 1984

Classification: Unclassifed

Please change Contract No. on cover to read: DAAK11-81-K0007.

Brenda C. Eckstein

BRENDA C. ECKSTEIN
Chief Technical Releases Section
Information Services Branch
Support Services Division
Research & Development Support
Directorate


DAT
FILM